Cell Stem Cell
Article

Unique and Independent Roles for MLL in Adult Hematopoietic Stem Cells and Progenitors

Craig D. Jude,[1] Leslie Climer,[1] Diyong Xu,[1] Erika Artinger,[1] Jill K. Fisher,[2,3] and Patricia Ernst[1,*]
[1]Department of Genetics and Norris Cotton Cancer Center, Dartmouth Medical School, 725 Remsen, HB7400, Hanover, NH 03755, USA
[2]Howard Hughes Medical Institute
[3]Department of Cancer Immunology and AIDS, Dana-Farber Cancer Institute Boston, MA 02115, USA
*Correspondence: patricia.ernst@dartmouth.edu
DOI 10.1016/j.stem.2007.05.019

SUMMARY

The *Mixed Lineage Leukemia* (*MLL*) gene is essential for embryonic hematopoietic stem cell (HSC) development, but its role during adult hematopoiesis is unknown. Using an inducible knockout model, we demonstrate that *Mll* is essential for the maintenance of adult HSCs and progenitors, with fatal bone marrow failure occurring within 3 weeks of *Mll* deletion. *Mll*-deficient cells are selectively lost from mixed bone marrow chimeras, demonstrating their failure to self-renew even in an intact bone marrow environment. Surprisingly, HSCs lacking *Mll* exhibit ectopic cell-cycle entry, resulting in the depletion of quiescent HSCs. In contrast, *Mll* deletion in myelo-erythroid progenitors results in reduced proliferation and reduced response to cytokine-induced cell-cycle entry. Committed lymphoid and myeloid cells no longer require *Mll*, defining the early multipotent stages of hematopoiesis as *Mll* dependent. These studies demonstrate that *Mll* plays selective and independent roles within the hematopoietic system, maintaining quiescence in HSCs and promoting proliferation in progenitors.

INTRODUCTION

To maintain the adult hematopoietic system, an ongoing and flexible interplay between lineage-instructive transcription factors and epigenetic regulators is likely to play a central role in determining appropriate numbers of each cell type. Several sequence-specific transcriptional regulators have been shown to play important roles in hematopoiesis, but the role of chromatin-modifying epigenetic regulators in this process is less clear. Polycomb (PcG) and trithorax (trxG) family proteins first identified in *Drosophila melanogaster* influence target gene expression in a manner that is heritable through multiple daughter cell divisions (Cavalli and Paro, 1998; Cavalli and Paro, 1999), making these proteins uniquely qualified to influence cell identity and plasticity during development or to regenerate tissues such as the hematopoietic system.

The *Mixed Lineage Leukemia* (*MLL*) gene was the first *trxG* gene identified as a proto-oncogene (Djabali et al., 1993; Domer et al., 1993; Gu et al., 1992; Tkachuk et al., 1992). Chromosomal translocations disrupting the *MLL* gene are primarily associated with acute lymphocytic (ALL) or myelogenous leukemia (AML) of infants, as well as secondary AML, accounting for more than 70% of each these two groups (reviewed in Biondi et al., 2000; Pui and Relling, 2000). *MLL* fusion genes produced by chromosomal translocation encode proteins composed of the N-terminal ~1/3 of MLL fused to one of over 50 identified translocation partners. The expression of MLL fusion proteins can influence lineage fidelity within the hematopoietic system (Drynan et al., 2005) and can produce cells with mixed lineage identity in human leukemia (Armstrong et al., 2002).

Retroviral expression of MLL fusion proteins in bone marrow cells is sufficient to produce AML or ALL in the mouse, as is the expression of MLL fusions by knockin or cre-mediated de novo chromosomal translocation (Ayton and Cleary, 2001; Daser and Rabbitts, 2005). The retroviral transduction model enabled structure-function assays that identified motifs within the MLL N terminus and the fusion partner that are essential for transformation. Collectively, such experiments indicate that MLL fusion proteins act via a gain-of-function mechanism through the acquisition of ectopic transactivation or dimerization capacity (reviewed in Ayton and Cleary, 2001). The N-terminal portion of MLL is likely to play a large role in targeting the fusion proteins to many of the same loci regulated by endogenous MLL, as fusion proteins have been shown by chromatin immunoprecipitation (ChIP) to localize to at least some of the same regulatory sequences as full-length wild-type MLL (Milne et al., 2005; Xia et al., 2005) and increase expression of those target genes (Horton et al., 2005).

Recent advances in purifying native MLL and complexes from cell lines have yielded important insights into the mechanism by which MLL acts on its target genes. Such complexes harbor histone methylation, acetylation,

and chromatin remodeling activities (Milne et al., 2002; Nakamura et al., 2002; Wysocka et al., 2005; Yokoyama et al., 2004). The Su(var)3-9/Enhancer of zeste/Trithorax (SET) domain at the extreme C terminus of MLL methylates histone H3 at lysine 4 (H3 K4), a modification associated with active transcription (Santos-Rosa et al., 2002). Consistent components of these complexes include WDR5, ASH2L, and menin. WDR5 and ASH2L interact with the C-terminal SET domain, acting as cofactors for the histone methyltransferase activity (Dou et al., 2006; Steward et al., 2006). Menin interacts with the MLL N terminus and bridges MLL to the basal transcriptional machinery (Yokoyama et al., 2004). The interaction of menin with the N terminus of MLL is important for maintaining expression of an endogenous MLL target gene in HeLa cells and is essential for transformation by MLL fusion proteins (Yokoyama et al., 2004, 2005). Other proteins have been described as part of the MLL complex, or as transient interactors, but scant in vivo data are available to validate the biological importance of these interactions.

To understand the mechanisms by which MLL fusion proteins are leukemogenic, it is critical to determine the normal function of MLL in vivo, particularly in the cell types that may represent the target for transformation by *MLL* oncogenes. Several groups have disrupted the *Mll* gene by different strategies, and in most cases, homozygous *Mll* mutants die during embryogenesis (Ayton et al., 2001; Yagi et al., 1998; Yu et al., 1995). Interestingly, the deletion of the SET domain alone is not lethal, but homozygous mutants exhibit mild loss-of-function phenotypes, including homeotic transformation and reduced expression of several *Hox* genes (Terranova et al., 2006).

Due to the embryonic lethality of most *Mll* mutants, studies aimed at identifying the role of *Mll* in the hematopoietic system have focused on embryonic hematopoiesis. Experiments using *Mll*-deficient embryonic stem (ES) cells demonstrated that these cells were incapable of differentiating into any hematopoietic cell types in adult animals or in the fetal liver. This multilineage block was due to the lack of HSCs in *Mll*-deficient embryos as measured functionally (Ernst et al., 2004a). Using an in vitro system, we showed that the block in hematopoietic development was accompanied by global reduction in *Hox* gene expression and could be rescued by the reintroduction of individual *Hox* genes (Ernst et al., 2004b). These experiments indicate that *Mll* plays an essential role in the development of definitive HSCs during embryogenesis and suggest that this is due to global *Hox* gene misexpression. However, the early and severe nature of the block in hematopoietic development precluded a detailed analysis of the mechanisms underlying the lack of HSCs or the assessment of *Mll* function in more differentiated hematopoietic lineages. To address these questions, we developed a mouse model in which *Mll* can be inducibly inactivated in the bone marrow and in specific lineages to provide a model system in which such functions could be studied in more detail.

RESULTS

Excision of *Mll* Exons 3 and 4 Generates a Loss-of-Function Allele

To create an inducible loss-of-function model for *Mll*, we designed an in-frame deletion to remove the AT hooks, nuclear targeting sequences (NTS), and subnuclear localization (SNL) sequences by flanking exons 3 and 4 with *loxP* sites ("floxed," Mll^{F}). Thus, cre recombinase-mediated excision produces an intragenic deletion ($Mll^{\Delta N}$), resulting in an MLL mutant protein lacking several NTS and other interaction motifs (Figure 1A). We recently introduced this allele into ES cells in combination with a strong loss-of-function allele (*Mll*-lacZ) and found that these cells exhibited a block in hematopoietic development (Ernst et al., 2004a) and a block in embryoid body hematopoiesis (Ernst et al., 2004b). Embryos homozygous for the $Mll^{\Delta N}$ allele died in utero at embryonic day 12.5, one day later in embryo development than $Mll^{\Delta N}$/*Mll*-lacZ and two days later than *Mll*-lacZ homozygotes (Figure S1 in the Supplemental Data available with this article online). $Mll^{\Delta N/+}$ animals exhibit normal viability and fertility and can be backcrossed to the C57Bl/6 strain without loss of heterozygote viability, in contrast to the exon 3 insertion *Mll*-lacZ strain (Yu et al., 1995). Thus, both the age of embryonic lethality and the hematopoietic phenotypes indicate that the $Mll^{\Delta N}$ allele is a strong hypomorphic allele of *Mll*, slightly less severe than the *Mll*-lacZ allele.

To confirm the predicted subcellular distribution of the $MLL^{\Delta N}$ protein, we expressed an N- and C-terminally tagged version of the predicted protein encoded by $Mll^{\Delta N}$ in 293T cells. MLL is processed by proteolytic cleavage to produce N- and C-terminal polypeptides that associate with each other within a large protein complex (Hsieh et al., 2003; Yokoyama et al., 2002). To determine the localization of both protein fragments, cells transfected with tagged wild-type and $MLL^{\Delta N}$ constructs were visualized by fluorescence microscopy using antibodies to the N- and C-terminal tags, as well as an internal MLL antibody that recognizes an epitope in the N-terminal fragment. $MLL^{\Delta N}$ was clearly excluded from the nucleus as determined by the N-terminal anti-Flag or anti-MLL antibodies, as well as the C-terminal anti-HA antibody (Figure 1B). In contrast, the full-length protein was exclusively nuclear as expected (Figures 1B and 1C). This subcellular localization was also observed with antibodies that detect the endogenous $MLL^{\Delta N}$ protein produced by cre-mediated *Mll* excision in $Mll^{F/F}$ bone marrow-derived macrophages (Figure 1C). Western blot analysis demonstrated similar levels of the $MLL^{\Delta N}$ protein compared to wild-type (data not shown).

To independently assess the function of the $MLL^{\Delta N}$ protein, we examined the expression of *Hoxa7*, *Hoxa9*, and *Hoxa10*, well-characterized MLL target genes, in $Mll^{\Delta N/\Delta N}$ hematopoietic cells. As shown in Figure 1D, we observed a progressive reduction (2- to ~50-fold) in *Hoxa7*, *Hoxa9*, and *Hoxa10* expression between days 6 and 11 after cre-mediated excision of *Mll*. Other *Hox* genes, such as *Hoxb3*, were not affected by *Mll* loss

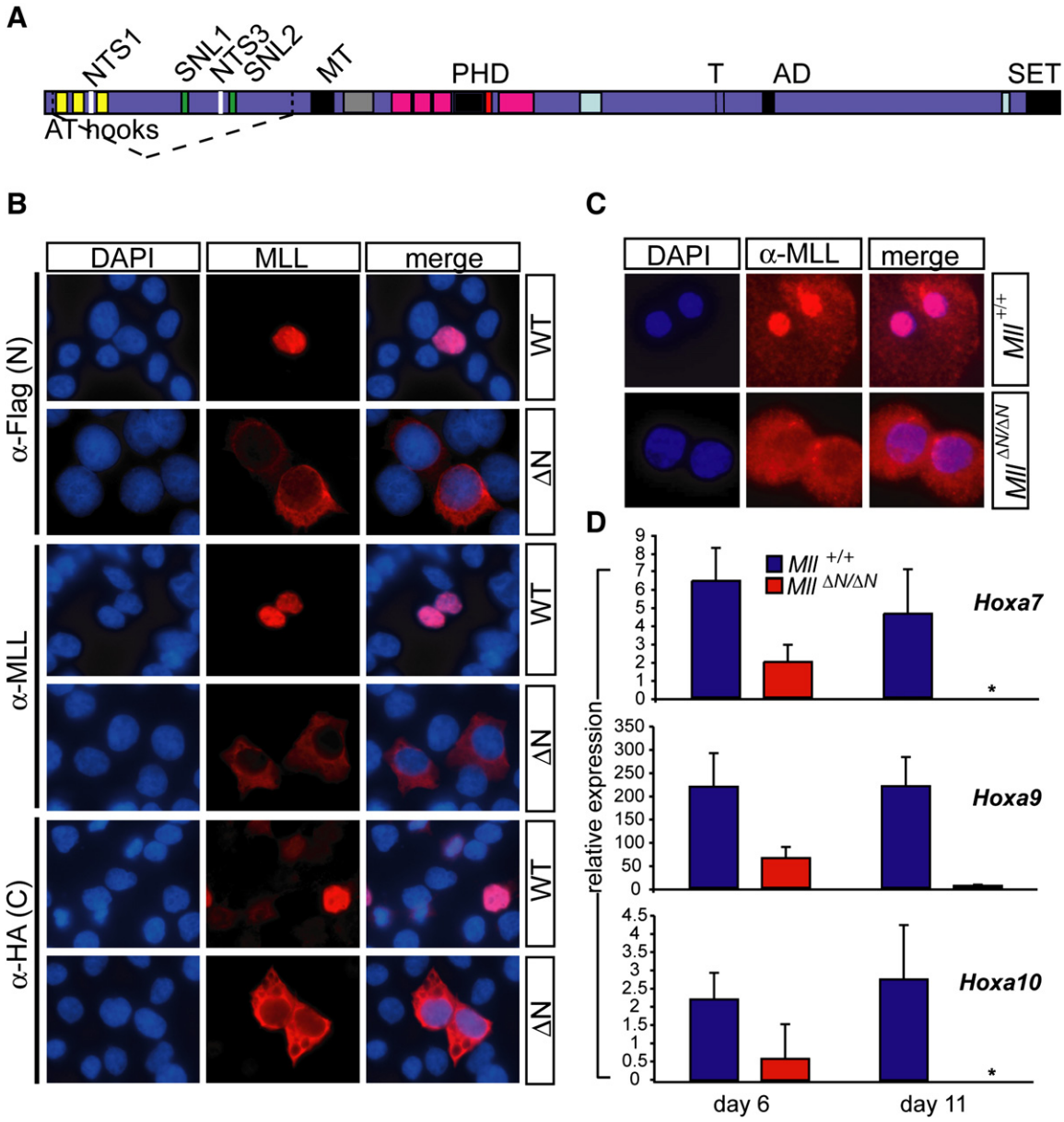

Figure 1. The *Mll*$^{\Delta N}$ Allele Encodes a Cytoplasmic Protein with Reduced Activity

(A) Diagram of wild-type MLL with the deletion of sequences encoded by exons 3 and 4 indicated by dashed lines. Homology motifs are shown as colored bars with the following indicated: AT hooks, minor groove DNA binding motif; SNL1 and 2, subnuclear targeting motif; NTS1 and 3, nuclear targeting signals; MT, DNA methyltransferase homology and CpG binding motif; PHD, plant homeodomain homology regions; T, taspase cleavage sites; AD, activation domain; and SET, Su(var)3-9/Enhancer of zeste/Trithorax homology region.

(B) Localization of tagged transfected wild-type MLL versus MLL$^{\Delta N}$. 293T cells were transfected with the construct labeled on the right of the panels and stained with antibodies indicated at the left. Examples shown are representative of three independent experiments.

(C) Subcellular localization of endogenous MLL in wild-type (upper panels) and *Mll*$^{\Delta N/\Delta N}$ macrophages (lower panels) derived in vitro from bone marrow cells.

(D) Relative *Hox* gene expression levels were determined by quantitative PCR using lin$^{neg/low}$ bone marrow cells isolated the days indicated after *Mll* deletion. Each bar represents the average expression level from at least three animals. Error bars represent the standard deviation of the average relative expression among animals. The asterisk denotes an undetectable Ct.

(Figure S2). Furthermore, highly purified c-Kit^{+}/lineage$^{neg/low}$/Sca-1^{+} (KLS) cells exhibited a similar fold reduction in *Hoxa* gene expression (Figure S3). Thus, excision of *Mll* exons 3 and 4 results in the production of a stable protein that fails to become imported into the nucleus and, based on the genetic, biochemical, and gene expression data above, results in a nonfunctional protein and a loss-of-function phenotype.

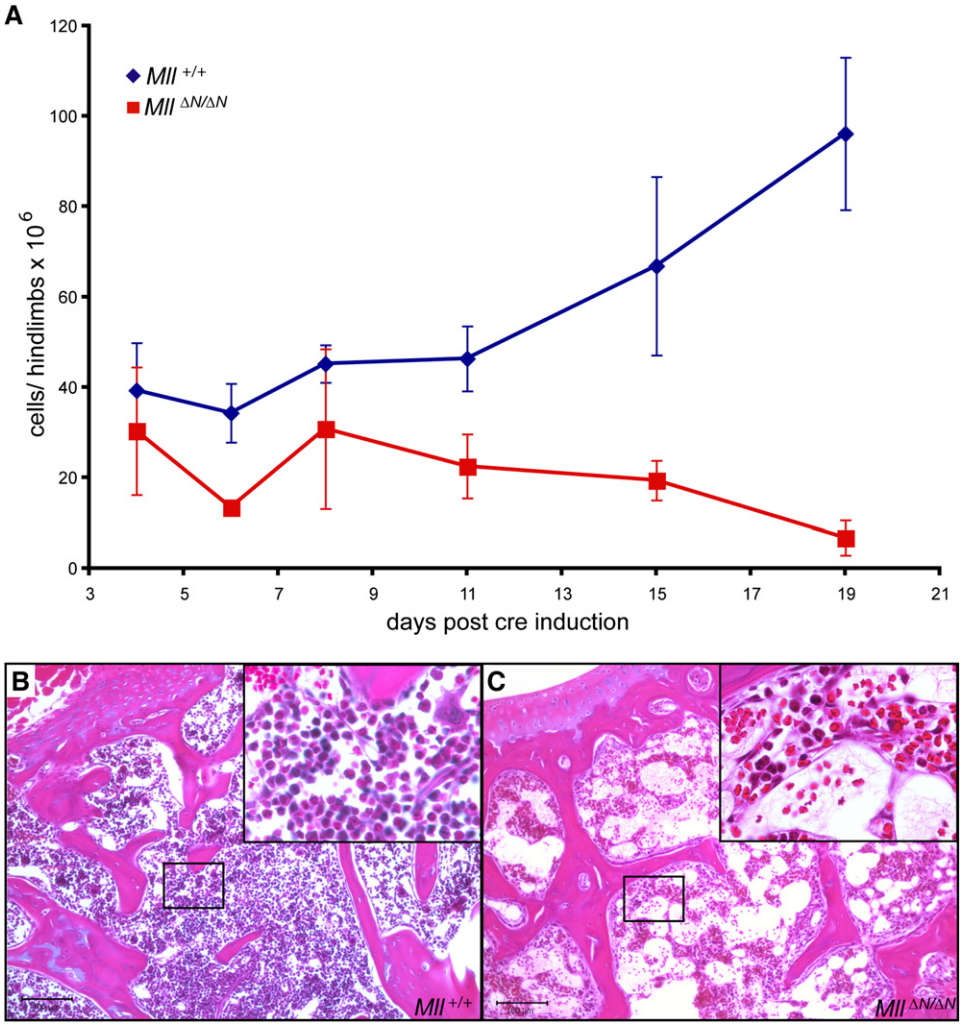

Figure 2. *Mll* Maintains Bone Marrow Homeostasis

(A) Average bone marrow cellularity per two hindlimbs as a function of time after the first pI:pC injection. Control animals (blue, $Mll^{+/+}$) represent pI:pC-injected *Mx1-cre;*$Mll^{+/+}$, and $Mll^{\Delta N/\Delta N}$ animals (red) represent pI:pC-injected *Mx1-cre;*$Mll^{F/F}$ animals. Error bars represent 95% confidence intervals. (B and C) Hematoxylin and eosin-stained sections from the humerus of control (B) or *Mx1-cre;*$Mll^{F/F}$ (C) animals 15 days after pI:pC injection. Slides were imaged at 100× and insets at 400× magnification.

Acute *Mll* Loss Results in Rapid Bone Marrow Failure

To determine the role of *Mll* during adult steady-state hematopoiesis, we employed an inducible transgenic cre mouse strain (*Mx1-cre*; Kuhn et al., 1995). Control and *Mx1-cre;*$Mll^{F/F}$ animals were subjected to a brief series of polyinosinic:polycytidylic acid (pI:pC) injections to induce cre-mediated excision of *Mll* in the bone marrow. Prior to pI:pC injection, bone marrow populations did not differ between control and *Mx1-cre;*$Mll^{F/F}$ animals (Figure S4). As early as 4 days after the first pI:pC injection, nearly all bone marrow cells had undergone cre-mediated excision (Figure S5). Approximately 19 days after inducing cre expression, animals in which 80% or more of the bone marrow expressed the $Mll^{\Delta N}$ allele exhibited bone marrow cytopenia and died or had to be sacrificed (Figure 2). The bone marrow of the few *Mx1-cre;*$Mll^{F/F}$ animals surviving the pI:pC injections was invariably composed of cells that had not undergone cre-mediated *Mll* excision (data not shown). *Mx1-cre;*$Mll^{F/F}$ pI:pC-injected animals that were also injected with wild-type bone marrow cells were healthy beyond 6 months (data not shown), demonstrating that the cause of death was from bone marrow failure.

The Maintenance of Adult HSCs Requires Continuous MLL Function

We previously demonstrated that MLL was essential for the development of HSCs in the embryo, so we first determined whether acute loss of *Mll* affected the HSC-enriched KSL population in the bone marrow. Phenotypic and functional analyses were performed from day 4 after

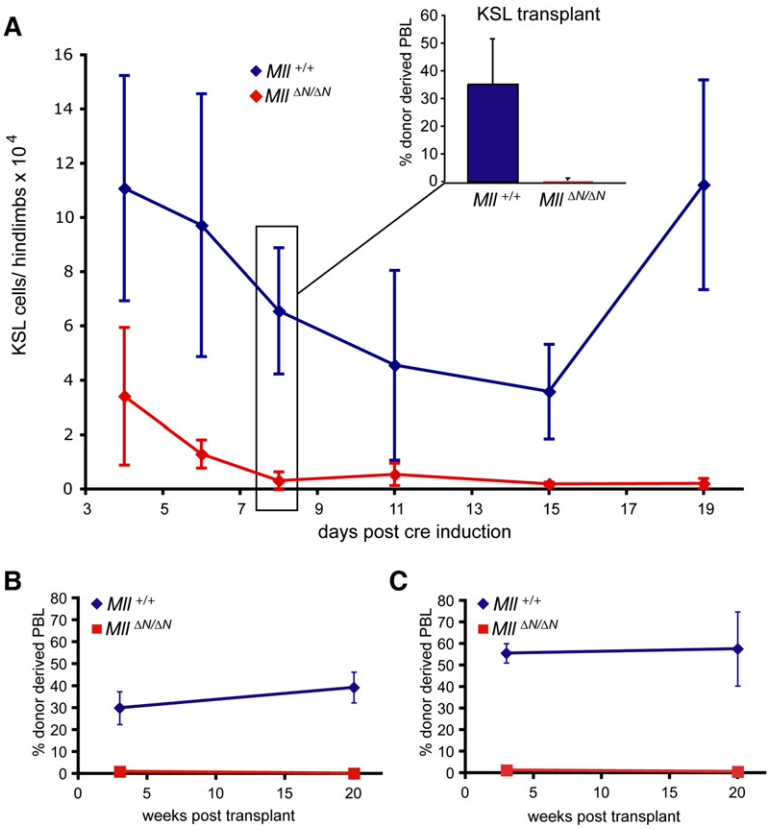

Figure 3. Loss of HSCs upon *Mll* Deletion

(A) Total KSL cell number per two hindlimbs of control (*Mx1-cre;Mll*$^{+/+}$ or *Mll*$^{F/F}$, blue) or *Mx1-cre;Mll*$^{F/F}$ (red) animals over a 2 week time course. Inset graph shows the results of competitive transplantation assays with 10,000 purified KSL cells to engraft lethally irradiated recipients. The donor cells were purified from *Mll*$^{+/+}$ (blue) or *Mll*$^{\Delta N/\Delta N}$ (red) bone marrow from animals 8 days after pI:pC treatment. For sorting details, see Figure S6. Peripheral blood contribution was determined 3 weeks after transplantation.

(B) Percentage of Ly5.1 (donor) peripheral blood leukocytes (PBLs) in lethally irradiated recipients transplanted with control (blue) or *Mll*$^{\Delta N/\Delta N}$ (red) unfractionated bone marrow cells from animals as described in (A). Donor cells were harvested at day 4 after pI:pC injection and were mixed with an equal number of wild-type Ly5.2 carrier cells.

(C) Donor contribution as in (B) using a 10:1 ratio of donor to carrier cells to engraft irradiated recipients. In both experiments, 3 × 10^5 wild-type carrier cells were used. For each set of experiments, 2–4 individual donors and 4–12 recipients were analyzed.

cre-mediated *Mll* deletion until the point at which *Mx1-cre;Mll*$^{F/F}$ animals died. Notably, the number of KSL cells dropped precipitously and failed to recover (Figure 3A). To determine whether the reduction in KSL cells reflected a cell-intrinsic defect, we performed competitive transplantation experiments with sorted pooled cells from the day 8 time point. We injected up to 10,000 viable KSL cells purified by fluorescence-activated cell sorting (FACS) from pI:pC-treated *Mx1-cre;Mll*$^{F/F}$ or control animals into lethally irradiated recipients. Animals injected with wild-type KSL cells all exhibited donor-derived cells in the peripheral blood; however, *Mll*$^{\Delta N/\Delta N}$ KSL cells failed to yield any significant donor contribution as early as 3 weeks after transplantation (Figure 3A, inset) or as late as 20 weeks (data not shown).

To determine whether HSC activity was present independent of the cell-surface phenotype, unfractionated *Mll*$^{\Delta N/\Delta N}$ bone marrow cells were tested in competitive transplantation experiments. We tested either equal numbers (1:1) or a 10-fold excess (10:1) of *Mll*$^{\Delta N/\Delta N}$ bone marrow mixed with wild-type bone marrow cells (Figures 3B and 3C). Remarkably, even a 10-fold excess of *Mll*$^{\Delta N/\Delta N}$ cells yielded recipients that were engrafted exclusively by wild-type cells (Figure 3C). Thus, *Mll* deletion results in the rapid decline in a phenotypically-defined HSC-enriched population and loss of HSC activity from this population and, in fact, from the bone marrow in general.

Consequences of *Mll* Deletion on HSC Viability and Proliferation

One explanation for the inability of *Mll*$^{\Delta N/\Delta N}$ KSL to compete with wild-type cells in transplantation experiments, as well as their disappearance from conditional knockout bone marrow, is that cells undergo programmed cell death in response to *Mll* deletion. In fact, an *Mx1-cre*-induced knockout of the antiapoptotic *Mcl-1* gene exhibits very similar kinetics of bone marrow cytopenia and HSC loss (Opferman et al., 2005). To determine whether cell death occurs in response to *Mll* loss, we assessed Annexin V and propidium iodide (PI) staining of KSL cells throughout the time course after *Mll* deletion. As shown in Figure 4A, we found no significant difference in the proportion of Annexin V$^+$ KSL cells at any time point. Annexin V$^+$ cells were detectable in other populations in the bone marrow, but there were no significant differences between the two genotypes in any population tested, nor was there a difference in the overall viability (PI$^+$) at early time points (day 0–11, data not shown).

Because programmed cell death did not account for the engraftment and homeostasis defects identified in *Mll*-deficient KSL cells, we considered growth arrest as an alternative hypothesis. For these experiments, we assessed the proportion of KSL cells in cycle by using 12 hr bromodeoxyuridine (BrdU) pulses (Figures 4B and 4C). Cell-surface staining was performed to identify KSL cells followed by intracellular staining for BrdU detection

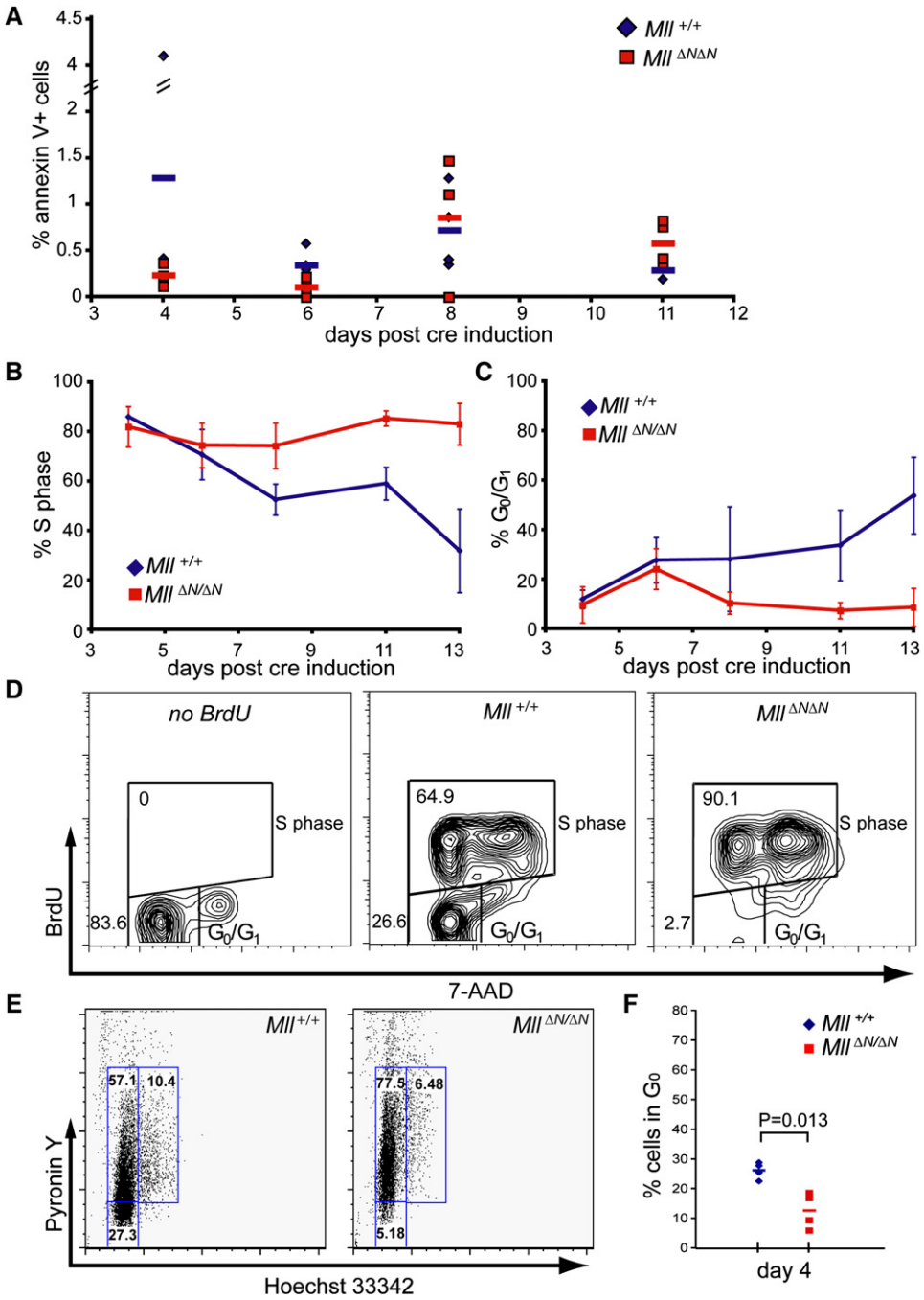

Figure 4. Cell Death and Proliferation within the *Mll*$^{\Delta N/\Delta N}$ KSL Population

(A) Control (blue) or *Mll*$^{\Delta N/\Delta N}$ (red) cells were stained with lineage, c-Kit, and Sca-1 antibodies and Annexin V to assess cell death within the KSL population over time. The percentage of Annexin V$^+$ cells within the KSL gated population is shown from individual animals with the average shown as a bar. For gating examples, see Figure S6B and S6C. Control (blue) or *Mll*$^{\Delta N/\Delta N}$ (red) cells were stained as above, fixed, and then stained with anti-BrdU and 7-AAD. Data in (B) indicate the percentage of BrdU-positive KLS cells from at least three individual animals per time point with the error bars representing 95% confidence intervals. Data in (C) represent the percentage of BrdU-negative KSL cells (G_0/G_1 gate, [D]).

(D) Representative FACS plots illustrating BrdU and 7-AAD staining of KSL cells 11 days post cre induction.

(E) Representative Hoechst/Pyronin staining of sorted KLS/CD48^{neg} cells at day 4 post cre induction, and (F) compiled Hoechst/Pyronin results from four individual animals per genotype based on the gates shown in (E). Similar results were obtained in at least three independent experiments.

(identifying cells in S phase during the prior 12 hr). Surprisingly, we found a significant increase in BrdU$^+$ KSL cells in *Mll*$^{\Delta N/\Delta N}$ bone marrow starting at day 8 after *Mll* deletion, becoming more severe by day 13 (Figure 4B). Conversely, there were almost no BrdU-negative cells in the *Mll*$^{\Delta N/\Delta N}$ KSL population from day 11 (Figures 4C and 4D). We

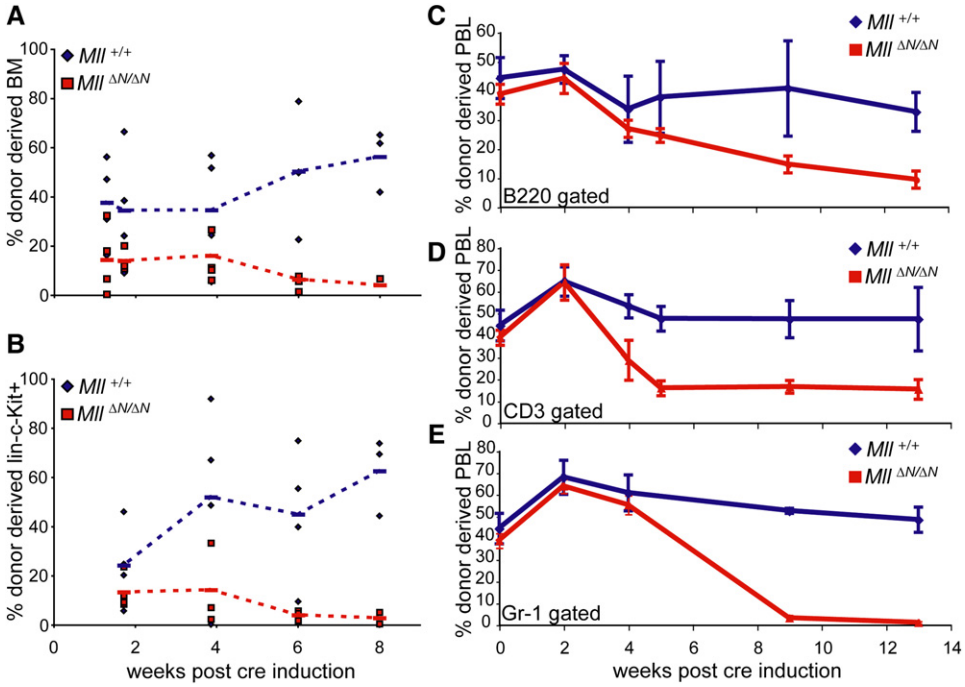

Figure 5. Selective Attrition of *Mll*$^{\Delta N/\Delta N}$ Cells from Mixed Bone Marrow Chimeras

(A) Percentage of donor-type cells (Ly5.1$^+$) within total bone marrow of chimeras. Bone marrow chimeras were established by coinjecting equal numbers of Ly5.1 donor bone marrow cells (from either *Mx1-cre;Mll*$^{+/+}$ or *Mx1-cre;Mll*$^{F/F}$ donors) plus wild-type bone marrow and waiting >6 weeks until stable engraftment. Chimeras were then injected four times with pI:pC, and complete excision of *Mll* was confirmed 2 weeks after the first injection.

(B) Percentage of donor cells (Ly5.1$^+$) within the lin$^{neg/low}$/c-Kit$^+$ gated population.

(C–E) Percentage of donor-derived PBLs gated on (C) B220 for B cells, (D) CD3 for T cells, and (E) Gr-1 for neutrophils. Blue diamonds, chimeras generated with *Mx1-cre;Mll*$^{+/+}$ cells, and red squares, chimeras generated with *Mx1-cre;Mll*$^{F/F}$ cells. Error bars represent the standard deviation.

further enriched HSCs from this population to examine the proportion of quiescent (G_0) cells by sorting CD48^{neg}/KSL cells (Kiel et al., 2005). Four days after cre induction (prior to the increase in S phase cells), we found that *Mll*$^{\Delta N/\Delta N}$ CD48^{neg}/KSL cells consistently exhibited a shift from G_0 to G_1 relative to control cells (Figures 4E and 4F). Therefore the first defect observed in *Mll*$^{\Delta N/\Delta N}$ HSCs is the failure to maintain quiescence, followed shortly thereafter by an increased number of cycling KSL cells. These data suggest that the depletion of HSCs upon *Mll* loss is due to their failure to self-renew and maintain a noncycling population of HSCs.

To determine whether *Mll*$^{\Delta N/\Delta N}$ HSCs and their progeny are ultimately depleted in vivo due to a failure to self-renew, we generated chimeric animals in which cotransplanted wild-type bone marrow supports long-term animal viability. Bone marrow chimeras were generated with Ly5.2$^+$ wild-type cells mixed with either Ly5.1$^+$ *Mx1-cre*;*Mll*$^{F/F}$ or Ly5.1$^+$ transgene-negative *Mll*$^{F/F}$ cells. After pI:pC treatment, the *Mx1-cre*;*Mll*$^{F/F}$ (now *Mll*$^{\Delta N/\Delta N}$) cells were selectively lost from chimeras (Figure 5). This loss occurred first in the bone marrow, with the lin$^{neg/low}$/c-Kit$^+$ pool depleted of *Mll*$^{\Delta N/\Delta N}$ cells by 6 weeks (Figures 5A and 5B), followed shortly after by a decline in *Mll*$^{\Delta N/\Delta N}$ neutrophils, B-, and T cells in the peripheral blood (Figures 5C–5E). Because whole bone marrow was transferred, the fact that peripheral blood T- and B cells were not completely depleted (Figures 5C and 5D) likely reflects the long half-life of these cells (>12 weeks; Forster and Rajewsky, 1990; Kondo et al., 1997), whereas the more rapid and complete loss of *Mll*$^{\Delta N/\Delta N}$ neutrophils (half-life of 1 to 2 days) reflects the complete exhaustion of *Mll*$^{\Delta N/\Delta N}$ HSCs. These data demonstrate that *Mll*-deficient HSCs are completely depleted, even in a bone marrow environment that includes wild-type neighboring hematopoietic cells and does not become cytopenic. However, these data do not account for the rapid cell loss in pI:pC-injected *Mx1-cre*;*Mll*$^{F/F}$ animals (Figure 2A). To investigate this further, we focused on the consequences of *Mll* deletion on progenitor populations.

Mll Plays an Independent Role in Maintaining Progenitor Pools

To determine whether lineage-committed progenitors were also affected by the loss of MLL function, we analyzed representative myeloid and lymphoid progenitor populations by cell-surface phenotype. We found that the absolute number of common lymphocyte progenitors (CLP), common myeloid progenitors (CMP), granulocyte-macrophage progenitors (GMP), and megakaryocyte-erythrocyte progenitors (MEP) was reduced 1.4- to 4-fold by day 11 after *Mll* deletion (Figure 6A). This was

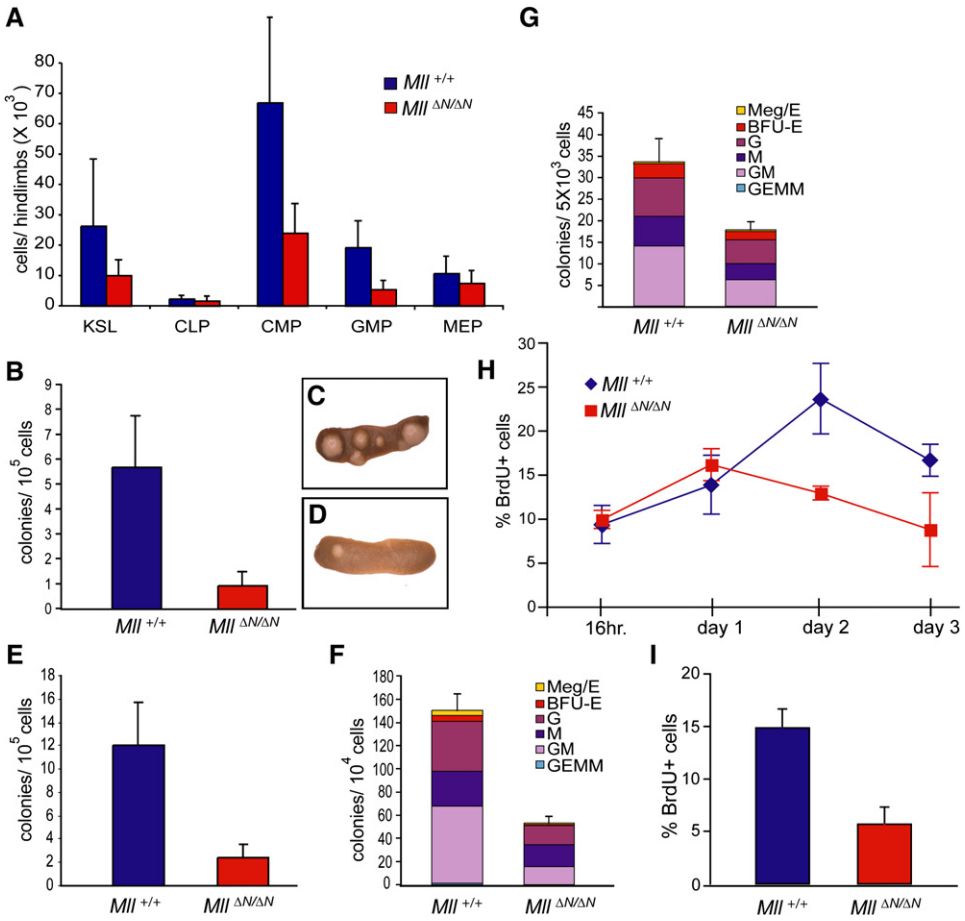

Figure 6. Reduction in Lymphoid and Myeloid Progenitors upon *Mll* Deletion

(A) Average cell number per two hindlimbs at day 11 post cre induction for the indicated cell types: c-Kit$^+$/lineage$^{neg/low}$/Sca-1$^+$, KLS; common lymphocyte progenitors, CLP; common myeloid progenitors, CMP; granulocyte-megakaryocyte progenitors, GMP; and megakaryocyte-erythroid progenitors, MEP. Averages are from three to four animals, and error bars represent 95% confidence intervals.

(B) Colonies per spleen (CFU-S$_8$) produced from pI:pC-injected control (*Mll*$^{F/F}$, blue) or *Mx1-cre*;*Mll*$^{F/F}$ donors (red). Donor cells (1 × 10^5) were harvested from animals 4 days after cre induction. At least four donor animals and 16 irradiated recipients were used per genotype. Error bars represent 95% confidence intervals.

(C and D) Representative spleens for *Mll*$^{+/+}$ (C) or *Mll*$^{\Delta N/\Delta N}$ (D) donor cells.

(E) CFU-preB frequency in lin$^{neg/low}$ bone marrow. Control (*Mll*$^{F/F}$, blue) or *Mll*$^{\Delta N/\Delta N}$ cells (red) were generated as in (B) but were enriched in lin$^{neg/low}$ cells, plated, and scored (see Experimental Procedures). Error bars represent 95% confidence intervals.

(F) CFU-C assay using bone marrow cells prepared as in (E) but anti-IL7Rα and -Sca-1 were included in the lineage mix. Cells from at least three donors per genotype were plated in triplicate, and colonies were scored 7 days later. Represented are the averages from all replicates with error bars indicating the 95% confidence interval of the averages. Megakaryocyte/erythroid, Meg/E; burst formation unit-erythroid, BFU-E; granulocyte, G; macrophage, M; granulocyte/macrophage, GM; and granulocyte, erythroid, macrophage, megakaryocyte colony, GEMM.

(G) CFU-C assay using in vitro-produced *Mll*$^{\Delta N/\Delta N}$ bone marrow cells. Lin$^{neg/low}$ cells from *Mll*$^{+/+}$ or *Mll*$^{F/F}$ bone marrow were infected with a cre-IRES-GFP retrovirus, and 5000 GFP$^+$ cells were plated in methylcellulose in triplicate as described in (E). Error bars represent 95% confidence intervals.

(H) Lin$^{neg/low}$/IL7Rα^-/Sca-1$^-$ cells were enriched from control (*Mll*$^{F/F}$, blue) or *Mll*$^{\Delta N/\Delta N}$ (red) samples prepared as in (F) from animals 11 days after cre induction. Samples were cultured in liquid medium containing SCF, IL-3, and IL-6. Cells were pulsed for 1 hr with BrdU, harvested, and analyzed by flow cytometry at the indicated time points, reflecting days of in vitro culture. Error bars represent 95% confidence intervals.

(I) Cells as described above were incubated with low serum and cytokine-free medium overnight, followed by readdition of serum and cytokines for 1 hr followed by BrdU pulses as in (H). Error bars represent 95% confidence intervals.

predominantly due to an overall reduction in lin$^{neg/low}$/c-Kit$^+$ cells (3.8-fold, data not shown).

To examine progenitor frequencies prior to their phenotypic reduction, we subjected bone marrow from the day 6 time point to in vivo (colony-forming units-spleen day 8 [CFU-S$_8$]) and in vitro (colony-forming unit-culture [CFU-C]) clonal progenitor assays. Reduced myeloid, erythroid, and lymphoid colony frequencies were observed with *Mll*$^{\Delta N/\Delta N}$ bone marrow samples (2- to 5-fold, Figures 6B–6F). The reduction in all colony types suggests a uniform requirement for *Mll* in the primitive hematopoietic compartment.

The maintenance of progenitors in vivo may reflect an intrinsic requirement for *Mll* within the progenitor pool or

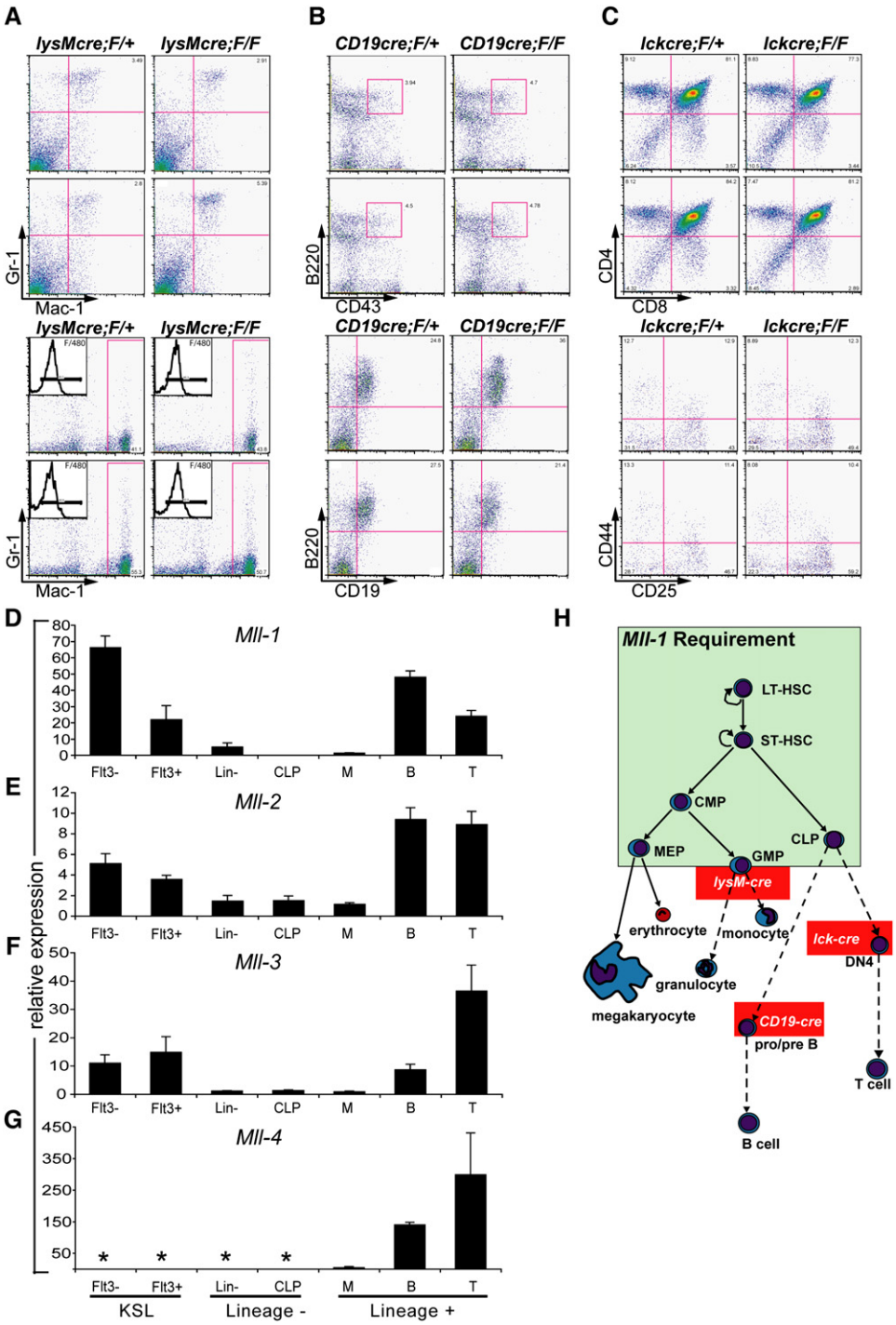

Figure 7. *Mll* Is Dispensable for Homeostasis of Lineage-Committed Cells and Is Not Compensated by Close Homologs in the Primitive Hematopoietic Compartment

(A) Analysis of bone marrow (top four panels) and peritoneal cells (bottom four panels) in *lysozyme M-cre*;*Mll*$^{F/+}$ (left column) and *lysozyme M-cre*;*Mll*$^{F/F}$ animals (right column). Inset in the lower four panels indicates F/480 expression on Mac-1/Gr-1 gated cells.

(B) Analysis of bone marrow cells of *CD19-cre*;*Mll*$^{F/+}$ (left column) and *CD19-cre*;*Mll*$^{F/F}$ (right column) animals.

(C) Analysis of thymocytes in *lck-cre*;*Mll*$^{F/+}$ (left column) and *lck-cre*;*Mll*$^{F/F}$ (right column) animals. The lower four panels represent CD4^{-}/CD8^{-} gated cells stained with the indicated antibodies. Two representative animals are shown for each strain.

(D–G) The expression of *Mll* homologs within purified hematopoietic populations. Quantitative real-time PCR results are shown for *Mll* (*Mll-1*) (D), *Mll-2* (E), *Mll-3* (F), and *Mll-4* (G). Populations are as described in Figure 6, with KSL cells further fractionated to enrich HSCs with short- and long-term engrafting potential (Flt3^{+} and Flt3^{-}, respectively). Also tested are the populations predicted to be affected in the lineage-specific cre strains:

a prior effect in generating progenitors from HSCs. To distinguish between these possibilities, we excised *Mll* in myelo-erythroid progenitors (lin$^{neg/low}$/Sca-1^{-}/IL-7Rα^{-} cells) purified from *Mll*$^{F/F}$ or *Mll*$^{+/+}$ bone marrow and determined CFU-C frequencies with *Mll*$^{\Delta N/\Delta N}$ cells generated in vitro through retroviral introduction of cre recombinase. This approach also revealed ~2-fold reduced CFU-C from *Mll*$^{\Delta N/\Delta N}$ myelo-erythroid progenitors, with all colony types similarly reduced (Figure 6G). Together, these data indicate that *Mll* is required for the maintenance of myelo-erythroid progenitors through a cell-intrinsic mechanism.

Proliferation Defects in *Mll*$^{\Delta N/\Delta N}$ Myelo-Erythroid Progenitors

To determine the basis for the functional and phenotypic reduction in *Mll*$^{\Delta N/\Delta N}$ progenitors, we assessed cell death and proliferation. We found no significant difference between the viability of *Mll*$^{\Delta N/\Delta N}$ cells in vivo or using the in vitro cre excision strategy described above (data not shown). We assessed proliferation in vitro by using a pool of myelo-erythroid progenitors (lin$^{neg/low}$/IL7Rα^{-}/c-Kit^{+}/Sca-1^{-} cells encompassing the CMP, GMP, and MEP populations). Using a time course of in vitro BrdU pulses, we found that *Mll*$^{\Delta N/\Delta N}$ progenitors exhibited reduced proliferation relative to controls (Figure 6H). In addition, serum/cytokine starvation experiments demonstrated that *Mll*$^{\Delta N/\Delta N}$ progenitors exhibited a 2.6-fold reduction in cells that could re-enter the cell cycle upon serum and cytokine restoration (Figure 6I). Importantly, the composition of the cell populations before or after in vitro culture was not significantly different between wild-type and *Mll*$^{\Delta N/\Delta N}$ populations (Figure S7 and data not shown). Based on these results, we conclude that *Mll* is required to sustain cytokine-driven proliferation of myelo-erythroid progenitors. Thus, the combination of ectopic, nonrenewing HSC proliferation in conjunction with the reduced proliferation within the larger progenitor pool (lin$^{neg/low}$/c-Kit^{+}) is likely to play a major role in the rapid attrition of cells in the pI:pC-injected *Mx1-cre*;*Mll*$^{F/F}$ animals.

Differentiating T-, B-, and Myeloid Cells No Longer Require *Mll* for Homeostasis

To determine whether *Mll* is continuously required throughout the differentiation of myeloid and lymphoid cells, we used lineage-specific cre transgenic or knockin strains to delete *Mll* in cells subsequent to lineage commitment. In contrast to the results with more primitive progenitors, we found no difference in the steady-state number or function of peripheral B cells, T cells, or macrophages and neutrophils in *CD19-cre*, *lck-cre*, or *lysozyme-M cre*;*Mll*$^{F/F}$ animals, respectively (data not shown). We carefully examined the populations representing the beginning of maximal cre expression in each strain and found that there were no differences in cell number or phenotype despite efficient gene deletion within the appropriate population (Figures 7A–7C and data not shown). Thus, these data delineate an early window of hematopoietic development as *Mll* dependent, encompassing the stem and progenitor pools. These data also demonstrate that our failure to detect mature *Mll*$^{\Delta N/\Delta N}$ leukocytes in transplanted animals (Figures 3 and 5) was not due to a late block in T cell, B cell, or granulocyte differentiation, and therefore accurately reflect a defect in stem/progenitor function.

Due to the contrast of these results with the severe, multilineage phenotype observed in early progenitors, we considered compensation by *Mll* homologs as an explanation for the differential effect of *Mll* deletion on primitive versus more mature, lineage-committed cell types. The *Mll* homologs *Mll-2* through *-4* exhibit similar domain organization and encode SET domains predicted to methylate histone substrates with the same specificity (FitzGerald and Diaz, 1999; Prasad et al., 1997; Ruault et al., 2002). *Mll-2*, the most closely related homolog, is expressed in a similar manner to *Mll* in the hematopoietic system (see below). MLL-2 has been isolated in similar protein complexes as MLL and has also been localized to the same target gene by ChIP (Dou et al., 2005; Hughes et al., 2004; Nakamura et al., 2002; Yokoyama et al., 2004). *Mll-1*, *-2*, *-3*, and *-4* are expressed in CD4^{+}CD8^{+} thymocytes and CD19^{+}B220^{+} pro/pre B cells, which were analyzed in the *lck-cre* and *CD19-cre* strains, respectively (Figures 7A–7G and Figure S8). The overlap in expression of *Mll* homologs illustrates the potential for compensatory functions within in these cell types; however, *Mll-2* and *-3* are also expressed significantly within the KSL population and thus would be equally capable to compensate for *Mll-1* loss in stem and progenitor populations, which is not the case.

These data demonstrate that the selective expression of *Mll* homologs within the hematopoietic system cannot account for the selective effects of *Mll-1* loss shown in this study. Despite the expression of *Mll-2* and *-3* within stem and progenitor populations, *Mll-1* performs an essential and nonredundant role in maintaining HSCs and progenitors (Figure 7H). In the more mature populations, it is possible that the relatively high levels of *Mll-2*, *-3*, and *-4* compensate for *Mll-1* loss, but a definitive test of this hypothesis will require the analysis of compound mutants.

DISCUSSION

The central finding of this study is that adult steady-state hematopoiesis depends on *Mll*, based on essential

myelomonocytic precursors (M, Mac-1^{+}/Gr-1^{+}), pro/pre-B cells (B, B220^{+}/CD19^{+}), and double-positive T cells (T, CD4^{+}/CD8^{+}). Results represent the mean of triplicate reactions with all expression levels normalized to *Gapdh*. Error bars indicate standard deviation, and asterisks indicate an undetectable Ct. Similar results were obtained in three independent experiments.

(H) Model illustrating the essential, nonredundant role of MLL in maintaining stem and progenitor cells. The green box encompasses cells affected by MLL loss, with those outside the box unaffected at the level of steady-state cell numbers. Red boxes indicate point at which lineage-specific cre expression occurs using the strains shown.

functions performed within hematopoietic stem and progenitor cells. In the absence of *Mll*, HSCs exit from a quiescent state and precociously undergo cell-cycle entry. Ectopic cycling of HSCs occurs without an increase in this population and coincident with functional deficits, suggesting that cell division in this compartment is accompanied by differentiation and not self-renewal. In contrast, the role of *Mll* within primitive myelo-erythroid progenitors appears to be quite distinct, in that progenitor frequency is reduced upon *Mll* deletion through a mechanism involving reduced proliferation. In conjunction with germline loss-of-function analyses (Ernst et al., 2004a), the studies presented here demonstrate that *Mll* is necessary for both the development and maintenance of HSCs. Further characterization will reveal whether all of these MLL-dependent processes utilize common or distinct molecular pathways.

Our data generally support the concept that MLL acts on a selective set of target genes in different cell types. Based on a genome-wide ChIP study in the U937 cell line, it has been proposed that MLL functions as a transcription start site-specific global transcriptional regulator (Guenther et al., 2005). This conclusion is partly based on the large overlap in Pol II and MLL localization at active promoters. If this colocalization indicated a biologically important association, one would expect a severe consequence for all cells in which MLL activity is removed. This prediction is difficult to reconcile with the selective phenotypes observed in vivo upon *Mll* loss. For example, ES cells and many differentiating tissues in chimeric animals are unaffected by *Mll* deficiency (Ernst et al., 2004a; Ernst et al., 2004b). These observations, along with the results presented in this study, suggest that selective and distinct target genes are regulated by MLL and its homologs in different tissues.

The reduced proliferation of myelo-erythroid progenitors shown in this study is consistent with previous observations using embryoid body-derived hematopoietic progenitors. In these studies, the reduced expression of multiple *Hox* genes appeared to be the primary cause for the reduced colony frequency in *Mll* mutant embryoid bodies (Ernst et al., 2004b). Thus, we predict that the reduced *Hox* gene expression in progenitors is similarly likely to play a major role in reduced progenitor frequency and proliferation upon *Mll* deletion. Conversely, *Hoxa7* and *Hoxa9* are consistently overexpressed in MLL fusion-initiated leukemia in humans and in mouse models, and are rate limiting for leukemogenesis or influential in determining leukemic cell phenotype (Armstrong et al., 2002; Ayton and Cleary, 2003; Kumar et al., 2004; So et al., 2004). Based on the results of the current study and results of *Hox* expression analyses in *Mll* loss- and gain-of-function experiments (Ernst et al., 2004b; Horton et al., 2005), we propose that altered *Hox* gene expression may be responsible for the proliferation component of the leukemogenic program induced by MLL fusion proteins.

The regulation of quiescence in HSCs is less likely to be explained by *Hox* gene maintenance alone, based on analyses of individual and compound *Hox* gene knockouts in which such a phenotype has not been reported (Bijl et al., 2006; Brun et al., 2004; Lawrence et al., 2005). This suggests that there are other HSC-specific *Mll* target genes involved in this process. Such HSC-specific target genes may remain activated by MLL fusion oncoproteins as HSCs differentiate, resulting in the maintenance of a self-renewal program coincident with a proliferation-promoting program mediated by *Hox* gene overexpression. Candidate genes for this self-renewal program include those reported as reactivated in an MLL-AF9 leukemia model (Krivtsov et al., 2006). Leukemia can be initiated by introducing *MLL* fusion oncogenes into committed progenitors (Cozzio et al., 2003; Krivtsov et al., 2006; Somervaille and Cleary, 2006), suggesting that the reactivation of such a self-renewal program by *MLL* fusion oncogenes can occur in progenitors. However, the introduction of *MLL* fusion oncogenes into HSCs rather than progenitors may facilitate fusion protein access to a quiescence-promoting gene expression program. One prediction of this hypothesis is that the introduction of *Mll* fusions into HSCs (rather than progenitors) would result in a more persistent, chemotherapy-resistant pool of leukemic cells, a concept that has not been tested in mouse models.

Importantly, our studies suggest that targeting *MLL* fusion oncogenes through mechanisms that generally interfere with MLL function may cause bone marrow failure. Thus it will be essential to identify strategies that selectively target MLL fusion oncoproteins without compromising wild-type MLL function. This effort will be aided by a comprehensive assessment of target genes affected by MLL fusions versus those affected by wild-type MLL.

EXPERIMENTAL PROCEDURES

Mice, Competitive Transplantation, and CFU-S Assays

Animals were maintained in accord with the Dartmouth Animal Resources Center and I.A.C.U.C. policies. *Mll* floxed alleles and ES targeting have been described (Ernst et al., 2004a). To generate $Mll^{\Delta N}$ animals, $Mll^{F/F}$ animals were crossed to the *EIIa-cre* strain (Jackson Labs). $Mll^{\Delta N/\Delta N}$ embryos were generated by crossing heterozygotes. Eight a.m. of the day of vaginal plug observation was considered E 0.5. The $Mll^{F/F}$ strain was backcrossed to C57Bl/6 for more than nine generations then backcrossed to B6.SJL (Jackson Labs) for five generations. Animals were crossed to the *Mx1-cre*, *lysozyme M-cre*, *CD19-cre* (obtained from Drs. Rajewski and Orkin, Harvard Medical School) and *lck-cre* strains (obtained from Dr. Wilson, University of Washington) to produce homozygous *Mll* floxed ($Mll^{F/F}$), cre-expressing strains. *Mx1-cre*;$Mll^{F/F}$, *Mx1-cre*;$Mll^{+/+}$, or $Mll^{F/F}$ mice were treated with two to four injections of pI:pC (GE Healthcare) every other day. Two, three, or four injections were performed for the day 4, 6, or 8–19 time points, respectively. Increasing the number of injections resulted in a higher penetrance of the phenotypes described, without altering the kinetics of their appearance. All animals were 6–12 weeks old for analyses in this study. The following formula was used for the pI:pC dose: (10 × animal mass [g] + 50) μg pI:pC.

For competitive transplantation experiments, C57BL/6J recipients were irradiated with a split dose of 1100 Rads 3 hr apart. Bone marrow cells were prepared by crushing with a mortar and pestle in ice-cold Hank's buffered saline solution (HBSS) supplemented with 2% fetal bovine serum (FBS). Red cells were removed with ACK lysis buffer (0.15 M NH_4Cl, 10 mM $KHCO_3$, 0.1 mM EDTA [pH 7.2]). Bone marrow chimeras were generated by injecting a mixture of 1.25×10^6 donor cells (*Mx1-cre*;$Mll^{F/F}$, $Mll^{F/F}$, or *Mx1-cre*; $Mll^{+/+}$, Ly5.1) plus 2.5×10^5

carrier cells (wild-type Ly5.2 or Ly5.1/5.2) and waiting >6 weeks for stable engraftment. Animals were maintained on sterile food and water (containing 50 μg/mL Baytril) for 3 weeks after irradiation. For the CFU-S_8 assay, 1 × 10^5 bone marrow cells from animals receiving 2 pI:pC doses were injected into lethally irradiated recipients. Eight days later, spleens were transferred to Tellesniczky's fixative. Colonies were counted and photographed with a Leica MZ7.5 dissecting microscope fitted with a Cannon Powershot S3 IS digital camera.

Flow Cytometry, Annexin V Binding Assays, and G_0/G_1 Analysis

Lineage staining was accomplished with unconjugated rat anti-CD4, -CD3, -CD8, -Gr-1, -B220, -CD19, -Ter119, and -Mac-1 and for some experiments anti-Sca-1 and -IL-7Rα (all antibodies were from BD Biosciences except the IL7Rα [eBiosciences]). Lineage antibodies were detected with goat ant-rat $F(ab')_2$ tricolor (Caltag), blocked with rat serum (Sigma), and stained with anti-Sca-1 and -c-Kit antibodies (BD Biosciences). Stained cells were incubated with Annexin V FITC as described by the manufacturer and analyzed immediately with a FACSCalibur (BD Biosciences) and FlowJo software (Treestar, Inc). We first determined that *Mx1-cre;Mll*$^{+/+}$ and *Mll*$^{F/F}$ animals exhibited indistinguishable levels of Annexin V and PI staining after pI:pC injection (data not shown) then used either genotype as controls for the following experiments. Annexin V-positive controls were generated for each analysis by incubating cells with 1 mM H_2O_2 at 37°C for 5 min. G_0/G_1 analysis was performed by first FACS purifying KLS/CD48^{neg} cells then incubating 10,000 sorted cells in 10 μg/mL Hoechst 33342 and 100 μM verapamil (both from Molecular Probes) for 45 min at 37°C. Samples were then supplemented to 2 μg/mL Pyronin Y (Sigma), incubated for an additional 15 min, washed, and analyzed immediately on a FACSAria (BD Biosciences). Anti-CD48 was from BD Biosciences. The unpaired t test was used to evaluate the statistical significance of differences in G_0 populations.

In Vivo Proliferation Assays

Mx1-cre;Mll$^{F/F}$, *Mx1-cre;Mll*$^{+/+}$, or *Mll*$^{F/F}$ mice were pI:pC injected as described above. At 12 and 6 hr prior to sacrifice, animals were injected with 1 mg BrdU. Cells were harvested and stained as described above. Stained cells were then fixed, permeabilized, and incubated with FITC-labeled anti-BrdU and 7-AAD per the manufacturer's suggestions (BD Biosciences).

Ex Vivo Introduction of Cre Recombinase and In Vitro Progenitor Assays

Bone marrow cells were prepared from 6- to 8-week-old *Mll*$^{+/+}$ and *Mll*$^{F/F}$ mice. Cells were stained with unlabeled antibodies as described above and depleted with sheep anti-rat magnetic beads (Dynal). Lin$^{neg/low}$ cells were then resuspended in growth medium (IMDM containing 20% FBS, 200 mM nonessential amino acids [NEAA], 200 mM L-glutamine [L-gln], 100 U/ml penicillin G, 100 μg/ml streptomycin [P/S], and 50 μM 2-ME) supplemented with 40 ng/ml IL-6, 20 ng/ml IL-3, 40 U/ml LIF, 80 ng/ml SCF, and 10 μg/ml polybrene. Spin infection was performed for 30 min at 25°C in 96-well plates. FACS-purified GFP$^+$ cells were subjected to colony assays as described (Ernst et al., 2004b). For the proliferation assays, lin$^{neg/low}$ cells were enriched as described above from *Mx1-cre;Mll*$^{F/F}$ or *Mll*$^{F/F}$ animals at day 11 post cre induction. Cell densities were adjusted to 5 × 10^5 cells/mL in growth medium supplemented with 1XBIT (StemCell Technologies), 50 ng/mL SCF, 10 ng/mL IL-3, and 10 ng/mL IL-6. Cells were incubated with BrdU at 10 μM for 1 hr. For the starvation experiment, cells were grown for 2 days, washed and incubated in cytokine-free, 0.5% FBS growth medium overnight, shifted to complete medium, and then pulsed with BrdU as described above. For the pre-B colony assay, 10,000 lin$^{neg/low}$ cells were plated in Methocult M3630 (StemCell Technologies) supplemented with 100 ng/mL SCF, 20 ng/mL murine Flt3L, and 10 ng/mL IL-7. Pre-B colonies were scored after 7 days. Cytokines were from R&D Systems.

Real-Time, Quantitative PCR

Total RNA from the sorted populations indicated in Figure 7 was purified with the RNeasy Mini kit (QIAGEN). After extraction, 1 μg MS2 bacteriophage RNA (Roche) was added as a carrier, and mRNA was amplified with the RiboAmp RNA Amplification Kit (Arcturus) per the manufacturer's recommendations for one round of amplification. *Hox* gene detection was performed as described (Ernst et al., 2004b), and *Mll* family primer and probes are shown in Figure S5. Relative expression levels were determined by using the ΔΔCt method (Livak and Schmittgen, 2001) with data from triplicate multiplexed reactions normalized to *Gapdh*. Quantitative real-time PCR was performed on a 7900HT machine using the 9600 emulation setting (Applied Biosystems).

Histopathology

For bone marrow sections, the humerus was removed, cleaned, and transferred to Bouin's fixative overnight at 4°C. Fixed samples were sectioned and stained by the Harvard Histopathology Core Facility. Samples were imaged on a Nikon Optiphot-2 microscope with 10× and 40× objectives.

Plasmids

The region spanning the exon 3 to 4 deletion (ΔN) was amplified by PCR from *Mll*$^{\Delta N/\Delta N}$ fibroblast RNA. This PCR product was inserted into the FseI and PvuI sites of the human MLL cDNA. The resulting MLL$^{\Delta N}$ cDNA was modified to encode the Flag epitope at the 5′ end and the HA epitope at the 3′ end by inserting annealed oligonucleotides encoding the epitope sequence. The tagged cDNAs (wild-type and MLL$^{\Delta N}$) were then subcloned into pCDNA3.1(−) (Invitrogen) at the XhoI and EcoRV sites.

Cell Culture, Transfection, and Immunofluorescence

293T cells were maintained in DMEM supplemented with 10% FBS, 200 mM L-gln, P/S, and 100 nM NEAA and transfected with FuGENE 6 (Roche). Thirty-six hours posttransfection, cells were plated on coverslips and grown overnight before fixing in 4% paraformaldehyde in PBS for 5 min. Cells were then blocked with PBS containing 2% goat serum and 0.2% Triton X-100 overnight. Anti-Flag M2 (1:100, Sigma), anti-MLL1 (BL1290), and anti-HA (both 1:100, Bethyl Labs) were incubated with coverslips for 30 min at room temperature, then washed three times in PBS. Detection was performed with Alexa Fluor-568 goat anti-mouse or Alexa Fluor-488 goat anti-rabbit (both at 1:1000, Molecular Probes). Stained cells were then washed three times in PBS, with the final wash containing 1μg/mL 4′, 6-diamidino-2-phenylindole (DAPI). Coverslips were mounted onto slides with Prolong Gold antifade medium (Molecular Probes). Images were captured with a Zeiss AxioVisionZ1 microscope and analyzed in Adobe Photoshop. Macrophages were cytospun onto slides and stained as described above.

Supplemental Data

Supplemental Data include eight figures and can be found with this article online at http://www.cellstemcell.com/cgi/content/full/1/3/324/DC1/.

ACKNOWLEDGMENTS

This study is dedicated to Stanley Korsmeyer, in whose lab the generation of the mouse model described here was initiated. This work was supported by funds from the Sydney Kimmel and V Foundations, NCRR COBRE grant #2P20RR016437, NIH #DK067119, and ACS IRG#82-003-21. We acknowledge the insightful comments of David Traver, Malek Djabali, and Iannis Aifantis. We are grateful for the gifts of cre mice from Drs. Rajewsky and Orkin. We thank Hanno Hock for essential advice on pI:pC vendors and Amy Wagers for advice on the Hoechst/Pyronin staining. We thank Gary Ward for expert cell sorting, Nancy Speck and her laboratory members for helpful comments,

R. Mako Saito for help with microscopy, and Victor Ambros and laboratory members for help with real-time PCR.

Received: February 8, 2007
Revised: April 15, 2007
Accepted: May 22, 2007
Published: September 12, 2007

REFERENCES

Armstrong, S.A., Staunton, J.E., Silverman, L.B., Pieters, R., den Boer, M.L., Minden, M.D., Sallan, S.E., Lander, E.S., Golub, T.R., and Korsmeyer, S.J. (2002). MLL translocations specify a distinct gene expression profile that distinguishes a unique leukemia. Nat. Genet. *30*, 41–47.

Ayton, P.M., and Cleary, M.L. (2001). Molecular mechanisms of leukemogenesis mediated by MLL fusion proteins. Oncogene *20*, 5695–5707.

Ayton, P.M., and Cleary, M.L. (2003). Transformation of myeloid progenitors by MLL oncoproteins is dependent on Hoxa7 and Hoxa9. Genes Dev. *17*, 2298–2307.

Ayton, P., Sneddon, S.F., Palmer, D.B., Rosewell, I.R., Owen, M.J., Young, B., Presley, R., and Subramanian, V. (2001). Truncation of the Mll gene in exon 5 by gene targeting leads to early preimplantation lethality of homozygous embryos. Genesis *30*, 201–212.

Bijl, J., Thompson, A., Ramirez-Solis, R., Krosl, J., Grier, D.G., Lawrence, H.J., and Sauvageau, G. (2006). Analysis of HSC activity and compensatory Hox gene expression profile in Hoxb cluster mutant fetal liver cells. Blood *108*, 116–122.

Biondi, A., Cimino, G., Pieters, R., and Pui, C.H. (2000). Biological and therapeutic aspects of infant leukemia. Blood *96*, 24–33.

Brun, A.C., Bjornsson, J.M., Magnusson, M., Larsson, N., Leveen, P., Ehinger, M., Nilsson, E., and Karlsson, S. (2004). Hoxb4-deficient mice undergo normal hematopoietic development but exhibit a mild proliferation defect in hematopoietic stem cells. Blood *103*, 4126–4133.

Cavalli, G., and Paro, R. (1998). The Drosophila Fab-7 chromosomal element conveys epigenetic inheritance during mitosis and meiosis. Cell *93*, 505–518.

Cavalli, G., and Paro, R. (1999). Epigenetic inheritance of active chromatin after removal of the main transactivator. Science *286*, 955–958.

Cozzio, A., Passegue, E., Ayton, P.M., Karsunky, H., Cleary, M.L., and Weissman, I.L. (2003). Similar MLL-associated leukemias arising from self-renewing stem cells and short-lived myeloid progenitors. Genes Dev. *17*, 3029–3035.

Daser, A., and Rabbitts, T.H. (2005). The versatile mixed lineage leukaemia gene MLL and its many associations in leukaemogenesis. Semin. Cancer Biol. *15*, 175–188.

Djabali, M., Selleri, L., Parry, P., Bower, M., Young, B., and Evans, G.A. (1993). A trithorax-like gene is interrupted by chromosome 11q23 translocations in acute leukaemias. Nat. Genet. *4*, 431.

Domer, P.H., Fakharzadeh, S.S., Chen, C.S., Jockel, J., Johansen, L., Silverman, G.A., Kersey, J.H., and Korsmeyer, S.J. (1993). Acute mixed-lineage leukemia t(4;11)(q21;q23) generates an MLL-AF4 fusion product. Proc. Natl. Acad. Sci. USA *90*, 7884–7888.

Dou, Y., Milne, T.A., Tackett, A.J., Smith, E.R., Fukuda, A., Wysocka, J., Allis, C.D., Chait, B.T., Hess, J.L., and Roeder, R.G. (2005). Physical association and coordinate function of the H3 K4 methyltransferase MLL1 and the H4 K16 acetyltransferase MOF. Cell *121*, 873–885.

Dou, Y., Milne, T.A., Ruthenburg, A.J., Lee, S., Lee, J.W., Verdine, G.L., Allis, C.D., and Roeder, R.G. (2006). Regulation of MLL1 H3K4 methyltransferase activity by its core components. Nat. Struct. Mol. Biol. *13*, 713–719.

Drynan, L.F., Pannell, R., Forster, A., Chan, N.M., Cano, F., Daser, A., and Rabbitts, T.H. (2005). Mll fusions generated by Cre-loxP-mediated de novo translocations can induce lineage reassignment in tumorigenesis. EMBO J. *24*, 3136–3146.

Ernst, P., Fisher, J.K., Avery, W., Wade, S., Foy, D., and Korsmeyer, S.J. (2004a). Definitive hematopoiesis requires the mixed-lineage leukemia gene. Dev. Cell *6*, 437–443.

Ernst, P., Mabon, M., Davidson, A.J., Zon, L.I., and Korsmeyer, S.J. (2004b). An Mll-dependent Hox program drives hematopoietic progenitor expansion. Curr. Biol. *14*, 2063–2069.

FitzGerald, K.T., and Diaz, M.O. (1999). MLL2: a new mammalian member of the trx/MLL family of genes. Genomics *59*, 187–192.

Forster, I., and Rajewsky, K. (1990). The bulk of the peripheral B-cell pool in mice is stable and not rapidly renewed from the bone marrow. Proc. Natl. Acad. Sci. USA *87*, 4781–4784.

Gu, Y., Nakamura, T., Alder, H., Prasad, R., Canaani, O., Cimino, G., Croce, C.M., and Canaani, E. (1992). The t(4;11) chromosome translocation of human acute leukemias fuses the ALL-1 gene, related to Drosophila trithorax, to the AF-4 gene. Cell *71*, 701–708.

Guenther, M.G., Jenner, R.G., Chevalier, B., Nakamura, T., Croce, C.M., Canaani, E., and Young, R.A. (2005). Global and Hox-specific roles for the MLL1 methyltransferase. Proc. Natl. Acad. Sci. USA *102*, 8603–8608.

Horton, S.J., Grier, D.G., McGonigle, G.J., Thompson, A., Morrow, M., De Silva, I., Moulding, D.A., Kioussis, D., Lappin, T.R., Brady, H.J., and Williams, O. (2005). Continuous MLL-ENL expression is necessary to establish a "Hox Code" and maintain immortalization of hematopoietic progenitor cells. Cancer Res. *65*, 9245–9252.

Hsieh, J.J., Ernst, P., Erdjument-Bromage, H., Tempst, P., and Korsmeyer, S.J. (2003). Proteolytic cleavage of MLL generates a complex of N- and C-terminal fragments that confers protein stability and subnuclear localization. Mol. Cell. Biol. *23*, 186–194.

Hughes, C.M., Rozenblatt-Rosen, O., Milne, T.A., Copeland, T.D., Levine, S.S., Lee, J.C., Hayes, D.N., Shanmugam, K.S., Bhattacharjee, A., Biondi, C.A., et al. (2004). Menin associates with a trithorax family histone methyltransferase complex and with the hoxc8 locus. Mol. Cell *13*, 587–597.

Kiel, M.J., Yilmaz, O.H., Iwashita, T., Yilmaz, O.H., Terhorst, C., and Morrison, S.J. (2005). SLAM family receptors distinguish hematopoietic stem and progenitor cells and reveal endothelial niches for stem cells. Cell *121*, 1109–1121.

Kondo, M., Weissman, I.L., and Akashi, K. (1997). Identification of clonogenic common lymphoid progenitors in mouse bone marrow. Cell *91*, 661–672.

Krivtsov, A.V., Twomey, D., Feng, Z., Stubbs, M.C., Wang, Y., Faber, J., Levine, J.E., Wang, J., Hahn, W.C., Gilliland, D.G., et al. (2006). Transformation from committed progenitor to leukaemia stem cell initiated by MLL-AF9. Nature *442*, 818–822.

Kuhn, R., Schwenk, F., Aguet, M., and Rajewsky, K. (1995). Inducible gene targeting in mice. Science *269*, 1427–1429.

Kumar, A.R., Hudson, W.A., Chen, W., Nishiuchi, R., Yao, Q., and Kersey, J.H. (2004). Hoxa9 influences the phenotype but not the incidence of Mll-AF9 fusion gene leukemia. Blood *103*, 1823–1828.

Lawrence, H.J., Christensen, J., Fong, S., Hu, Y.L., Weissman, I., Sauvageau, G., Humphries, R.K., and Largman, C. (2005). Loss of expression of the Hoxa-9 homeobox gene impairs the proliferation and repopulating ability of hematopoietic stem cells. Blood *106*, 3988–3994.

Livak, K.J., and Schmittgen, T.D. (2001). Analysis of relative gene expression data using real-time quantitative PCR and the 2(-Delta Delta C(T)). Methods *25*, 402–408.

Milne, T.A., Briggs, S.D., Brock, H.W., Martin, M.E., Gibbs, D., Allis, C.D., and Hess, J.L. (2002). MLL targets SET domain methyltransferase activity to Hox gene promoters. Mol. Cell *10*, 1107–1117.

Milne, T.A., Martin, M.E., Brock, H.W., Slany, R.K., and Hess, J.L. (2005). Leukemogenic MLL fusion proteins bind across a broad region

of the Hox a9 locus, promoting transcription and multiple histone modifications. Cancer Res. *65*, 11367–11374.

Nakamura, T., Mori, T., Tada, S., Krajewski, W., Rozovskaia, T., Wassell, R., Dubois, G., Mazo, A., Croce, C.M., and Canaani, E. (2002). ALL-1 is a histone methyltransferase that assembles a supercomplex of proteins involved in transcriptional regulation. Mol. Cell *10*, 1119–1128.

Opferman, J.T., Iwasaki, H., Ong, C.C., Suh, H., Mizuno, S., Akashi, K., and Korsmeyer, S.J. (2005). Obligate role of anti-apoptotic MCL-1 in the survival of hematopoietic stem cells. Science *307*, 1101–1104.

Prasad, R., Zhadanov, A.B., Sedkov, Y., Bullrich, F., Druck, T., Rallapalli, R., Yano, T., Alder, H., Croce, C.M., Huebner, K., et al. (1997). Structure and expression pattern of human ALR, a novel gene with strong homology to ALL-1 involved in acute leukemia and to Drosophila trithorax. Oncogene *15*, 549–560.

Pui, C.H., and Relling, M.V. (2000). Topoisomerase II inhibitor-related acute myeloid leukaemia. Br. J. Haematol. *109*, 13–23.

Ruault, M., Brun, M.E., Ventura, M., Roizes, G., and De Sario, A. (2002). MLL3, a new human member of the TRX/MLL gene family, maps to 7q36, a chromosome region frequently deleted in myeloid leukaemia. Gene *284*, 73–81.

Santos-Rosa, H., Schneider, R., Bannister, A.J., Sherriff, J., Bernstein, B.E., Emre, N.C., Schreiber, S.L., Mellor, J., and Kouzarides, T. (2002). Active genes are tri-methylated at K4 of histone H3. Nature *419*, 407–411.

So, C.W., Karsunky, H., Wong, P., Weissman, I.L., and Cleary, M.L. (2004). Leukemic transformation of hematopoietic progenitors by MLL-GAS7 in the absence of Hoxa7 or Hoxa9. Blood *103*, 3192–3199.

Somervaille, T.C., and Cleary, M.L. (2006). Identification and characterization of leukemia stem cells in murine MLL-AF9 acute myeloid leukemia. Cancer Cell *10*, 257–268.

Steward, M.M., Lee, J.S., O'Donovan, A., Wyatt, M., Bernstein, B.E., and Shilatifard, A. (2006). Molecular regulation of H3K4 trimethylation by ASH2L, a shared subunit of MLL complexes. Nat. Struct. Mol. Biol. *13*, 852–854.

Terranova, R., Agherbi, H., Boned, A., Meresse, S., and Djabali, M. (2006). Histone and DNA methylation defects at Hox genes in mice expressing a SET domain-truncated form of Mll. Proc. Natl. Acad. Sci. USA *103*, 6629–6634.

Tkachuk, D.C., Kohler, S., and Cleary, M.L. (1992). Involvement of a homolog of Drosophila trithorax by 11q23 chromosomal translocations in acute leukemias. Cell *71*, 691–700.

Wysocka, J., Swigut, T., Milne, T.A., Dou, Y., Zhang, X., Burlingame, A.L., Roeder, R.G., Brivanlou, A.H., and Allis, C.D. (2005). WDR5 associates with histone H3 methylated at K4 and is essential for H3 K4 methylation and vertebrate development. Cell *121*, 859–872.

Xia, Z.B., Popovic, R., Chen, J., Theisler, C., Stuart, T., Santillan, D.A., Erfurth, F., Diaz, M.O., and Zeleznik-Le, N.J. (2005). The MLL fusion gene, MLL-AF4, regulates cyclin-dependent kinase inhibitor CDKN1B (p27kip1) expression. Proc. Natl. Acad. Sci. USA *102*, 14028–14033.

Yagi, H., Deguchi, K., Aono, A., Tani, Y., Kishimoto, T., and Komori, T. (1998). Growth disturbance in fetal liver hematopoiesis of Mll-mutant mice. Blood *92*, 108–117.

Yokoyama, A., Kitabayashi, I., Ayton, P.M., Cleary, M.L., and Ohki, M. (2002). Leukemia proto-oncoprotein MLL is proteolytically processed into 2 fragments with opposite transcriptional properties. Blood *100*, 3710–3718.

Yokoyama, A., Wang, Z., Wysocka, J., Sanyal, M., Aufiero, D.J., Kitabayashi, I., Herr, W., and Cleary, M.L. (2004). Leukemia proto-oncoprotein MLL forms a SET1-like histone methyltransferase complex with menin to regulate Hox gene expression. Mol. Cell. Biol. *24*, 5639–5649.

Yokoyama, A., Somervaille, T.C., Smith, K.S., Rozenblatt-Rosen, O., Meyerson, M., and Cleary, M.L. (2005). The menin tumor suppressor protein is an essential oncogenic cofactor for MLL-associated leukemogenesis. Cell *123*, 207–218.

Yu, B.D., Hess, J.L., Horning, S.E., Brown, G.A., and Korsmeyer, S.J. (1995). Altered Hox expression and segmental identity in Mll-mutant mice. Nature *378*, 505–508.

Cell Stem Cell, Volume *1*

Supplemental Data

Unique and Independent Roles for MLL in Adult Hematopoietic Stem Cells and Progenitors

Craig D. Jude, Leslie Climer, Diyong Xu, Erika Artinger, Jill K. Fisher, and Patricia Ernst

Age of embryonic lethality of *Mll* $^{\Delta N/\Delta N}$ mutants.

embryo age (dpc)	homozygotes (live *Mll* $^{\Delta N/\Delta N}$ out of total)
E10.5	3/15 (20%)
E11.5	5/19 (26%)
E12.0	4/17 (26%)
E13.0	0/26
E13.5	0/17
E14.0	0/11
E15.0	0/6

Figure S1. Age of lethality for homozygous *Mll*$^{\Delta N/\Delta N}$ embryos. *Mll*$^{\Delta N/+}$ animals were intercrossed and embryo age was defined considering the day of plug observation (8 a.m.) as day 0.5 post-coitum (dpc). Pregnant females were sacrificed at the embryonic day indicated and viable embryos were scored based on cardiac contractions. All embryos were genotyped by Southern blot or the 3 primer assay presented in Fig. S5 using yolk-sac or limb bud genomic DNA.

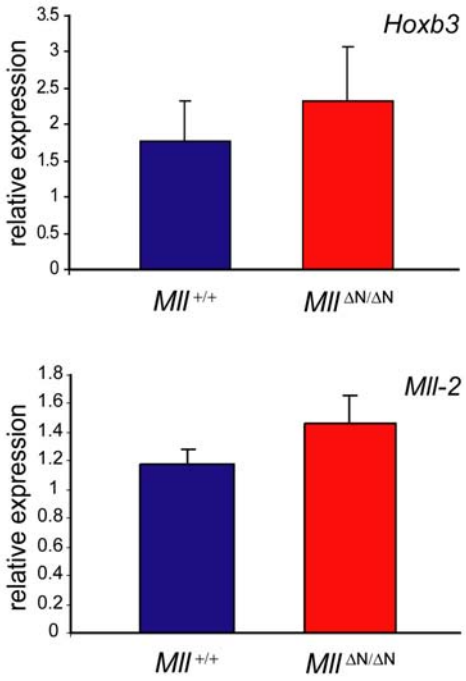

Figure S2. Expression of *Hoxb3* and *Mll-2* in lin$^{neg/low}$ bone marrow cells 11 days after cre induction as determined by quantitative real-time PCR. Error bars represent 95% confidence intervals.

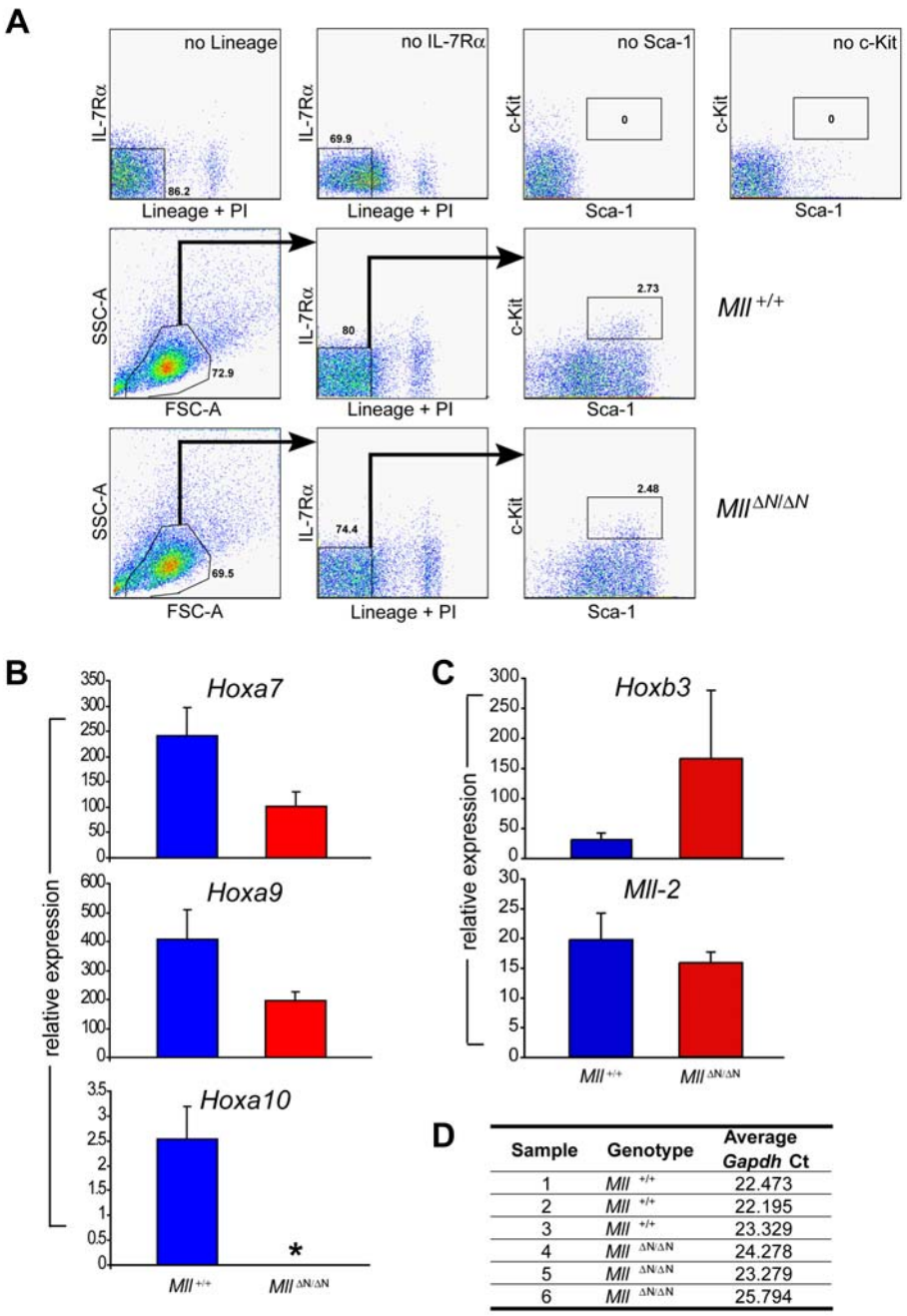

Sample	Genotype	Average *Gapdh* Ct
1	*Mll* $^{+/+}$	22.473
2	*Mll* $^{+/+}$	22.195
3	*Mll* $^{+/+}$	23.329
4	*Mll* $^{\Delta N/\Delta N}$	24.278
5	*Mll* $^{\Delta N/\Delta N}$	23.279
6	*Mll* $^{\Delta N/\Delta N}$	25.794

Figure S3. Expression of *Hox* genes in sorted KLS cells six days after cre induction. **A)** Gating used to sort KLS cells from bone marrow of $Mll^{+/+}$ and $Mll^{\Delta N/\Delta N}$ mice. Samples in which one antibody is withheld to demonstrate controls for positioning the gates are shown in the top row. Examples of $Mll^{+/+}$ and $Mll^{\Delta N/\Delta N}$ cells are shown in the bottom two rows. **B)** Results of quantitative real-time PCR assays using amplified RNA from sorted

KLS cells. Asterisk denotes undetectable expression. **C)** Expression of *Hoxb3* and *Mll-2* in sorted KLS cells as determined by quantitative real-time PCR. Error bars represent 95% confidence intervals. **D)** Table of raw *Gapdh* Ct values in the sorted KLS samples.

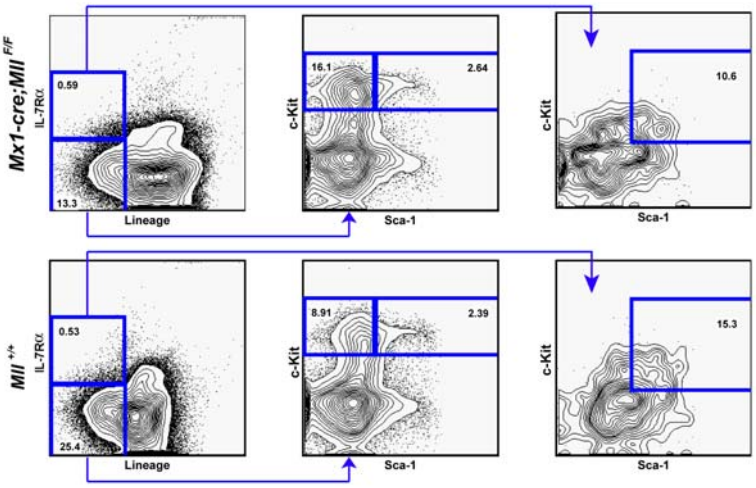

Figure S4. The FACS plots demonstrate the KSL and CLP gating for *Mx1-cre;Mll*$^{F/F}$(top row) and *Mll*$^{+/+}$samples (bottom row).

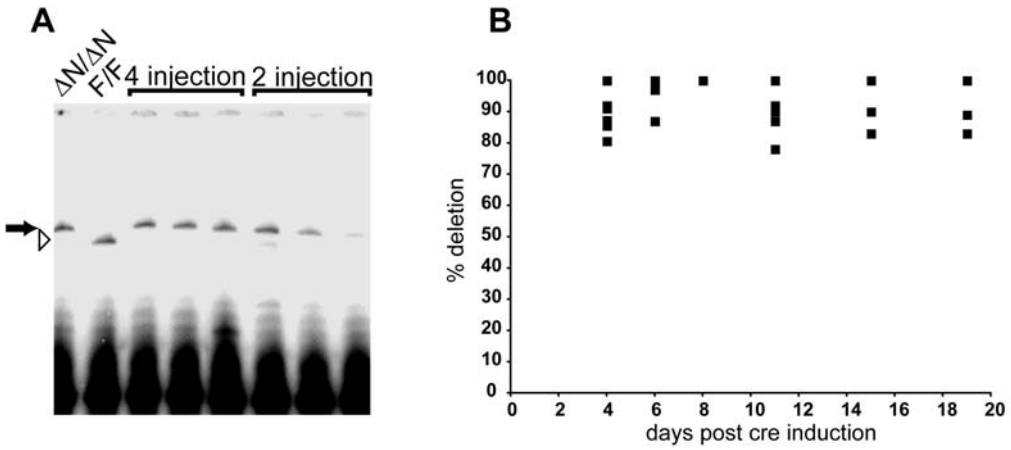

Figure S5. Efficiency of cre-mediated *Mll* deletion in bone marrow cells. **A)** Low-cycle PCR products using a ^{32}P-labeled forward primer were fractionated on an 8% acrylamide gel and visualized by autoradiography. The black arrow indicates the $Mll^{\Delta N}$ product and the open arrowhead indicates the Mll^{F} product. **B)** Quantification of *Mll* deletion efficiency in a subset of the individual mice used for Figure 3. PCR products were quantified by exposing dried gels to phosphorimager analysis to determine the relative ratio of $Mll^{\Delta N}$ versus Mll^{F} alleles. A standard curve was run for each experiment to ensure measurements in the linear range of the PCR reaction.

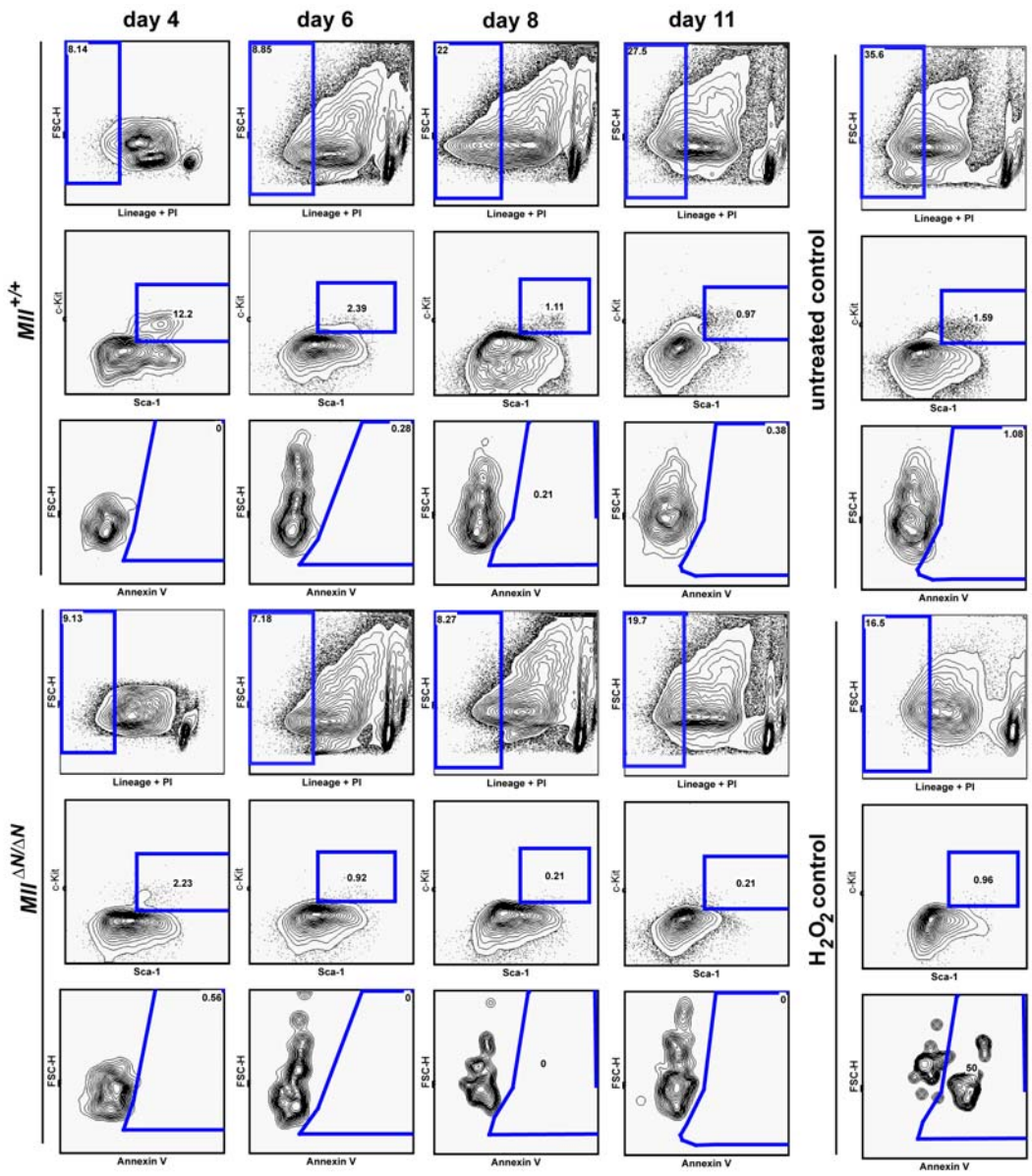

Figure S6. Representative examples of staining of *Mll*$^{+/+}$ and *Mll*$^{\Delta N/\Delta N}$ bone marrow samples used for the data shown in Fig 3A and 4A. Untreated control and H_2O_2-treated (annexin V positive control) analyses are shown in the final column.

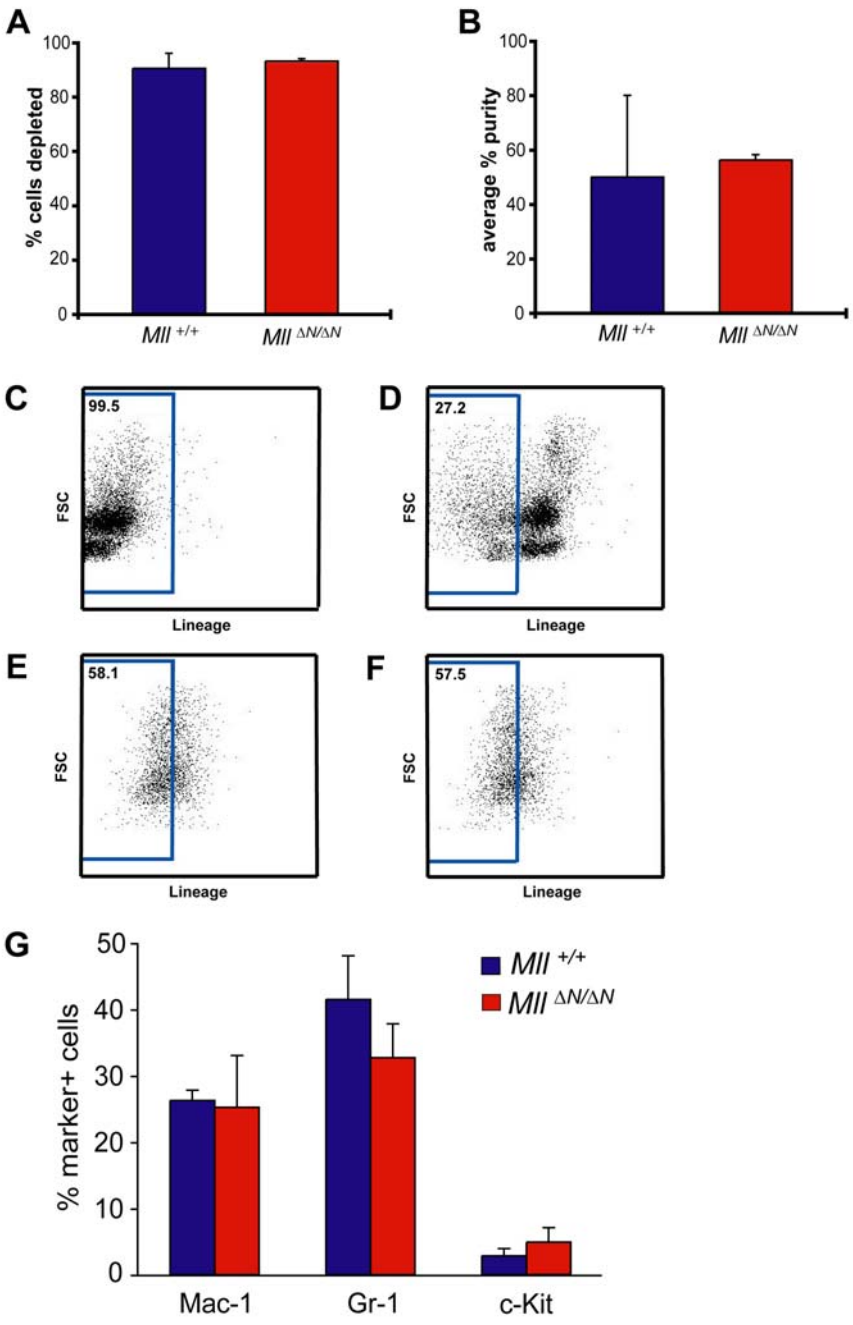

Figure S7 Composition of the cell populations before and after *in vitro* culture. The average percentage of **A)** cells depleted from crude bone marrow, and **B)** $lin^{neg/low}$ bone marrow cells after depletion of lineage-positive bone marrow cells. Percentages are shown for both genotypes. After depletion, cells were re-stained with a cocktail of lineage-specific antibodies (see Experimental Procedures) and detected with an anti-rat

fluorochrome conjugate. **C-D)** Gating used to identify myeloid progenitor cells. **C)** Unstained control. **D)** Lineage staining of crude bone marrow cells. Representative examples of progenitor cells enrichment of **E)** *Mll*$^{+/+}$, and **F)** *Mll*$^{\Delta N/\Delta N}$ cells after lineage depletion. **G)** Composition of the *in vitro* progenitor cultures after 5 days in SCF, IL-3 and IL-6 as described in the Experimental Procedures. Cells cultured in parallel with those used for the proliferation experiments were stained with the indicated antibodies and analyzed by flow cytometry. Total percentages of the indicated cells are shown for *Mll*$^{+/+}$(blue bars) or *Mll*$^{\Delta N/\Delta N}$ cells (red bars).

A

Design of MLL homolog TaqMan Primers and Probes							
					Amplicon		
Gene	Alternate Names	Accession # *	Location	Distance from 3' end	Length	Tm (C)	%GC
Mll1	*All-1, Htrx1, Mll*	02095	Spans Exons 33-34	3693 bp	96 bp	73	53.1
Mll2	*Wbp7, Trx2, Mll4*	06470	Spans Exons 33-34	809 bp	105 bp	73.5	55.2
Mll3		45291	Spans Exons 58-59	49 bp	106 bp	71.7	46.2
Mll4	*ALR, Mll2*	23741	Spans Exons 50-51	257 bp	81 bp	72.7	50.6

* Full form of accession number is ENSMUST000000xxxxx, only the last 5 digits are shown.

B

Sequence of MLL Homolog TaqMan Probes/Primers			
Gene		**Sequence**	**Annealing Temp. (C)**
Mll1	Forward Primer	5'-TGAGTACAACCCTAACGATGAGGAA-3'	60
	Reverse Primer	5'-CGGAATCTCATGGGCATTG-3'	
	Probe	5'-CGGAGGGCAACAAGCATGGATCTC-3'	
Mll2	Forward Primer	5'-TGCTGAGGTCTATCTCCGGAAGTGTA-3'	60
	Reverse Primer	5'-TCATCCTCTTCTTCATCACAGGTGGC-3'	
	Probe	5'-TTGACATGTTCAACTTCCTGGCCTCCCA-3'	
Mll3	Forward Primer	5'-AGCTCCAACCGGAGGATACAGAAA-3'	60
	Reverse Primer	5'-AGTTCACCGCTCCACAGTGACA-3'	
	Probe	5'-ACTTTGAAGATGACCAGCACAAGATTCCG-3'	
Mll4	Forward Primer	5'-AGTACATCGGCACCATCATTCGCA-3'	60
	Reverse Primer	5'-TGTAAATACCGCGGTTCTGCTCCT-3'	
	Probe	5'-ATGAGGTGGCCAATCGGCGGGAGAAA-3'	

C

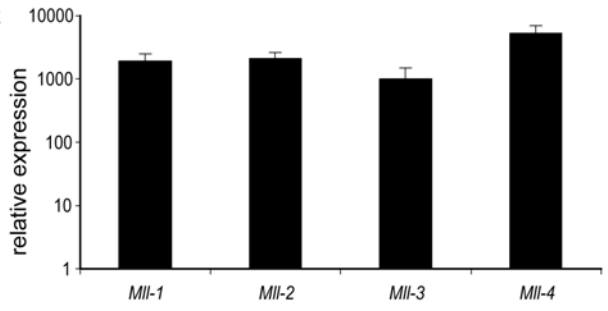

Figure S8. Design and characteristics of MLL homolog PCR primers and probes. **A)** Amplicon characteristics for the genes indicated. Gene nomenclature corresponds to our use in the text with alternate names shown. **B)** Primer and probe sequences. Probes were synthesized with 5'-FAM and 3'-TAMRA modifications. The default ABI cycling conditions were used for all reactions. **C)** Expression of MLL and homologs in testis. *Mll-1*, *Mll-2*, *Mll-3* and *Mll-4* gene expression levels in testis were determined as described in the Experimental Procedures and Fig. 7 legends. Results represent the mean expression level relative to *Gapdh* and displayed in log scale. A value of 1 is equal to the

level of *Mll-4* expression in the myelomonocytic population. Error bars represent standard deviation. Experiments were repeated at least three times with similar results.